HHS Public Access

Author manuscript

DNA Repair (Amst). Author manuscript; available in PMC 2021 February 01.

Published in final edited form as:

DNA Repair (Amst). 2020 February ; 86: 102769. doi:10.1016/j.dnarep.2019.102769.

The splicing component ISY1 regulates APE1 in base excision repair

Aruna S. Jaiswal[1,*], **Elizabeth A. Williamson**[1], **Gayathri Srinivasan**[1], **Kimi Kong**[1], **Carrie L. Lomelino**[2], **Robert Mckenna**[2], **Christi Walter**[3], **Patrick Sung**[4], **Satya Narayan**[5], **Robert Hromas**[1,*]

[1]–Division of Hemsatology and Medical Oncology, Department of Medicine, University of Texas Health Science Center, San Antonio, TX 78229.

[2]–Department of Biochemistry and Molecular Biology, University of Florida Health, Gainesville, FL 32610.

[3]–Department of Cell Systems and Anatomy, University of Texas Health Science Center, San Antonio, TX 78229.

[4]–Department of Biochemistry and Structural Biology, University of Texas Health Science Center, San Antonio, TX 78229; and Department of Molecular Biophysics and Biochemistry, Yale School of Medicine, New Haven, CT 06520.

[5]–Department of Anatomy and Cell Biology, University of Florida, Gainesville, FL 32610.

Abstract

The integrity of cellular genome is continuously challenged by endogenous and exogenous DNA damaging agents. If DNA damage is not removed in a timely fashion the replisome may stall at DNA lesions, causing fork collapse and genetic instability. Base excision DNA repair (BER) is the most important pathway for the removal of oxidized or mono-alkylated DNA. While the main components of the BER pathway are well defined, its regulatory mechanism is not yet understood. We report here that the RNA splicing factor ISY1 enhances apurinic/apyrimidinic endonuclease 1 (APE1) activity, the multifunctional enzyme in BER, by promoting its 5'−3' endonuclease activity. ISY1 expression is induced by oxidative damage, which would provide an immediate up-regulation of APE1 activity *in vivo* and enhance BER of oxidized bases. We further found that APE1 and ISY1 interact, and ISY1 enhances the ability of APE1 to recognize abasic sites in DNA. Using purified recombinant proteins, we reconstituted BER and demonstrated that ISY1 markedly promoted APE1 activity in both the short- and long-patch BER pathways. Our study identified

[*] Co-Corresponding authors: RH: Department of Medicine, UT Health San Antonio, University of Texas, 7703 Floyd Curl Dr., San Antonio, TX 78229; T-210-567-4432, F- 210-567-3435; hromas@uthscsa.edu. ASJ: Division of Hematology and Medical Oncology, Department of Medicine, University of Texas Health Science Center, 7703 Floyd Curl Dr., San Antonio, TX 78229; T-210-450-8647, jaiswala@uthscsa.edu.

Conflict of Interest: RH is on the board of directors and has equity in Dialectic Therapeutics, but this has no conflict of interest with the contents of this article.

ISY1 as an important regulator of the BER pathway, which would be of physiological relevance where suboptimal levels of APE1 are present. The interaction of ISY1 and APE1 also establishes a connection between DNA damage repair and pre-mRNA splicing.

Keywords

Base Excision Repair; Oxidative Stress; AP Endonuclease-1; RNA Splicing; ISY1

1. INTRODUCTION

DNA base modifications are the most common form of DNA damage. Such modifications can be caused by exposure to monofunctional alkylating agents and by endogenous oxidation, deamination or alkylation. More than 100 types of oxidative base modifications can potentially arise in DNA as a result of attack by reactive oxygen (ROS) and nitrogen species (1,2). These reactive chemical species are primarily generated by mitochondrial respiration or inflammation (3). DNA base damage can lead to DNA strand breaks and enhanced expression of proto-oncogenes (4,5). Cells are equipped with multiple pathways that efficiently repair damaged DNA and reverse the vast majority of genetic lesions formed during the life span of a cell (1,6,7). BER is a highly conserved pathway from bacteria to humans, and is capable of repairing most DNA alkylation, oxidation, deamination and depurination, as well as single-strand breaks (SSBs). BER is mediated through two sub-pathways designated short-patch (SP) BER, and multi-nucleotide (2–13 nucleotide repair patch) BER, also referred to as long-patch (LP) BER (8,9).

During BER, a DNA glycosylase recognizes the base lesion and then cleaves the N-glycosyl bond between the base and the sugar, producing an apurinic/apyrimidinic (AP) site. AP sites are cytotoxic and mutagenic, and can give rise to DNA-strand breaks by β-elimination (10). Spontaneous hydrolysis of the N-glycosidic bond also results in an AP site. Uracil occurs frequently in DNA after spontaneous deamination of cytosine and is removed by uracil-DNA glycosylase (11). Base damage occurs much more frequently at purines than pyrimidines. Most DNA damaging agents attack purines ten-fold more than pyrimidines; therefore, AP-sites in cellular DNA largely represent sites of purine loss (2).

APE1 not only functions in BER, but it also acts as a redox factor for maintaining transcription factors in a reduced active state (12,13). APE1 contains two functional domains: the C-terminal nuclease domain responsible for its DNA repair function, while its N-terminal domain is responsible for reduction/oxidation regulation. It protects against the oxidative stress, but which function plays a role is not clear. Under oxidative stress, APE1 stimulates the DNA binding capacity of several transcription factors, such as AP-1, NFκB, HIF-1a, and CREB (14). APE1 is elevated in many cancer types, such as ovarian, cervical, rhabdomyosarcoma, and germ-cell tumors (12), likely from the selective pressure of the oxidative stress associated with oncogenesis.

APE1 cleaves the DNA phosphodiester backbone immediately 5′ to an AP site (13,15–17) to generate a 3’ hydroxyl group and a 5’ sugar-phosphate moiety. During SP-BER, DNA polymerase β (POL β) removes the 5’ sugar-phosphate using its dRP-lyase activity and then

fills in the resulting one-nucleotide gap (18,19). The gap is sealed by LIG3/XRCC1 (20,21). XRCC1 is a multidomain scaffolding protein which interacts with number of repair proteins (22). XRCC1 stabilizes DNA ligase 3 and plays a role in SP-BER. Recent evidence indicates that DNA ligase1 rather than DNA ligase 3 plays a major role in both SN-BER and LP-BER in the nucleus, while DNA ligase 3's role is confined to mitochondria only (23,24). In LP-BER, PARP1 assists POL β in the displacement of the damaged DNA strand and fills in the resulting 2–20 nucleotide gap (5–7). Flap Endonuclease 1 (FEN1) cleaves the displaced DNA flap, and LIG1 seals the remaining nick (5–7). POL β is the primary polymerase involved in BER. Several other polymerases such as POL λ, POL δ and POL ε can participate in SP-BER or LP-BER (25–27). PCNA dependent LPBER pathway utilizes replicative DNA polymerases δ and /or ε. However, their involvement is tightly coupled to the cleavage of 5'-structure by FEN1 and sealing the gap by DNA ligase.

In both SP-BER and LP-BER, APE1 mediated cleavage of the AP site is a critical step (12, 13). However, the cellular selection of one BER pathway over the other depends mainly upon whether the residual deoxyribose at the AP site is oxidized or reduced. If that deoxyribose is oxidized or reduced then the AP site cannot be repaired by SP-BER pathway, and the cell chooses to repair only via the LP-BER pathway. If BER is not completed, cells accumulate APE1-induced DNA single strand breaks (SSBs) that a converging replication fork converts to double strand breaks, which can lead to replication fork collapse (28). These collapsed replication fork may lead to genome rearrangement or cell death.

In eukaryotes, precursor (pre) mRNA introns are removed from nascent transcripts by dynamic complexes called spliceosomes. Spliceosomes are composed of distinct subunits containing stable mRNA in tight association with multiple proteins. The spliceosome's conformation and composition changes throughout its assembly cycle (29,30). The spliceosome mediates two sequential steps of RNA transesterification for intron excision (31). Not all components of the spliceosome have been delineated. One estimate predicts more than 200 proteins are associated with human spliceosomes at various time during the splicing process (32). There are at least 141 proteins in the functional core complex (33–35). Spliceosome assembly is initiated by U1 and U2 small nuclear ribonuclear proteins (snRNPS) binding to the precursor mRNAs (pre-mRNAs) at 5' sites and branch-sites to yield a spliceosome complex (32). The first step, termed branching, usually results in release of the 5'-exon and formation of branched intron lariat intermediate followed by the second step, ligation of the 5'- and 3'-exons. At these steps, single-nucleotide precision is required; cells must have a mechanism to control the fidelity of pre-mRNA splicing or coding alterations would occur (36). The accuracy of nucleotide site recognition, nicking and re-ligation by the spliceosome resembles some aspects of BER. In addition, many of the proteins involved in splicing are phosphorylated after DNA damage by ATM and ATR (37). These observations suggest that splicing proteins could be repurposed by the cell to regulate the efficiency of DNA repair. We discovered that the splicing factor ISY1 interacts with APE1, and demonstrated that ISY1 directly enhances APE1's affinity for AP sites and its AP endonuclease activity. As such, ISY1 facilitates both SP-BER and LP-BER. Consistent with these biochemical findings, we provide biological evidence that ISY1 is needed for cell survival after treatment with agents that induce DNA base lesions that are eliminated via

BER. These data imply that ISY1 plays an important role in regulating the processing of abasic sites and thereby could preserve genomic stability.

2. MATERIALS AND METHODS

2.1. Cell lines and cell cultures

Human embryonic kidney cell line 293, human lung cancer cell lines A549, H157, and the prostate cancer cell line PC3 were grown in DMEM medium supplemented with 10% fetal bovine serum albumin and 100 U/ml of penicillin, and 100 μg/ml of streptomycin. The breast cancer cell line MCF7 was grown in MEM medium supplemented with 10% fetal bovine serum and penicillin and streptomycin antibiotics. Human colon cancer cell lines HCT-116 with a wild-type *APE1* gene or an APE1 gene-knockdown (kd) were grown in McCoy's 5a medium supplemented with 10% fetal bovine serum (FBS; Atlanta Biologicals, Atlanta, GA, USA). The HCT-116 cell line was obtained from the American Type Culture Collection (ATCC, Rockville, MD).

2.1.1 Cells Treatment—HCT116 control and APE knock-down cells were plated in complete media and allowed to grow to 60–70% confluence in 6-well plates. Cells were treated with MMS (0–1000 μM) and H_2O_2 (0–500 μM) for 10 h. After the treatment cells were trypsinized, washed and cell lysate prepared.

2.2. Transfection of HCT116 cells for ISY1 and APE1 knock-down

ISY1 and APE1 were transiently depleted in HCT-116 cells by using small interfering RNA (siRNA) and Lipofectamine RNAiMAX transfection Reagent (Life Technologies, USA). We used SMARTpool ON-TARGETplus and a non-target pool as siRNA controls. SiRNA for ISY1 and APE1 were purchased from Dharmacon (Lafayette, CO, USA). The nucleotide sequences of siRNA On-Target plus smart pool for ISY1 were:

ACACUGGGAGGUCCGGAUA,

GUUUAGGUGAAUUUCGAAU,

CAGAAGUAUGCAAGCGAGA, and

GAGCCGAGUUAGUGGAAAA.

The nucleotide sequences of siRNA On-Target plus smart pool for APE1 were:

CAAAGUUUCUUACGGCAUA,

GAGACCAAAUGUUCAGAGA,

CUUCGAGCCUGGAUUAAGA, and

UAACAGCAUAUGUACCUAA.

A day before transfection, HCT-116 cells were plated at the density 0.15×10^6 per well in a 6-well plate. The next day DNA:Lipid complex was prepared by mixing Lipofectamine

RNAi-Max and siRNA (20 nM for each) at the ratio of 3:1 of RNAi-Max and siRNA. DNA:Lipid complex was allowed to form for 30 min at room temperature. Cells were washed once with Opti-MEM and replaced with fresh Opti-MEM medium to remove serum and antibiotics. DNA:Lipid complex was added drop-wise to the cells. Cells were incubated with the complex for 8 h at 37°C followed by addition of 30% serum in Opti-MEM. Eight hours after transfection, 0.5 ml of 30% serum containing Opti-MEM medium was added to each well. Cells were harvested 48 hrs post-transfection, cell lysates were prepared and protein levels checked. Expression of ISY1 and APE1 were assessed by western blotting.

2.2.1 APE1 over-expression—APE1 was over expressed in HCT116 cells after knocking-down of ISY1 to see whether APE1 overexpression can rescue cells from MMS induced DNA damage. A day before transfection, HCT-116 cells were plated at the density 0.15×10^6 per well in a 6-well plate. Cells were transfected with ISY1-siRNA as described earlier. After 8–10 h of transient knock-down of ISY1-siRNA, APE1 was overexpressed using Flag-APE1 wt plasmid. DNA-lipid complex was assembled at room temperature by mixing 2 μg of Flag-APE1 wt plasmid with 6 μl of FuGENE 6 according to the recommended protocol of the manufacturer. After 36–48 h cells were exposed to 100 μM MMS for 30 min. MMS was removed and cells were supplemented with fresh medium and allowed to grow for various time. Cells were harvested at indicated time and processed for comet assay analysis. APE and ISY1 expression were confirmed by western blot analysis.

2.3. Oligonucleotides and chemicals

All oligonucleotides for electrophoretic mobility shift assay, *in vitro* nuclease and reconstitutive SP- and LP-BER assays were custom synthesized from Sigma-Genosys (Woodlands, TX). The nucleotide sequence of these oligonucleotides contained a uracil residue or an AP site analog, 3-hydroxy-2-hydroxymethyltetrahydrofuran (designated as F in the oligomers), both positioned at 24-nt. All the oligomers were PAGE (polyacrylamide gel electrophoresis) purified and reconstituted in TE buffer pH 8.0. T4-polynucleotide kinase (PNK) and Uracil DNA glycosylase were purchased from New England Bio labs (Ipswich, MA). Radionuclide [$\gamma-^{32}$P]ATP was purchased from Perkin Elmer, Inc. (Boston, MA). ISY1 and α-tubulin antibodies were purchased from Sigma Chemicals and APE1 antibody was purchased from Abcam (Cambridge, MA, USA). FEN1 and DNA Ligase 1 antibodies were purchased from Novus Biological (Centennial, CO, USA). Sequences of the custom synthesized oligo's from Sigma-Genosys are as follows:

Sense 63-mer U-DNA

5'-
CTAGATGCCTGCAGCTGATGCGC**U**GTACGGATCCACGTGTACGGTACCGAGGGCG
GGT CGAGA

Sense 63-mer F-DNA

5'-CTAGATGCCTGCAGCTGATGCGC**F**GTA

CGGATCCACGTGTACGGTACCGAGGGCGGGTCGAGA

Anti-sense 63-mer F-DNA

5’-
TCTCGACCCGCCCTCGGTACCGTACACGTGGATCCGTACGGCGCATCAGCTGCAG
GCAT CTAG

EMSA sense 37-mer F-DNA

5’-CCTGCAGCTGGTGCAAAAGT **F**ATTGCGGCGTGTACGGT

EMSA sense 37-mer control DNA

5’-CCTGCAGCTGGTGCAAAAGTATTGCGGCGTGTACGGT

EMSA anti-sense 37-mer DNA

5’-ACCGTACACGTTTCCTTACGGGGTCACCAGCTGCAGG

dRP Lyase sense 43-mer DNA

5’-TAGACTAGATGCCTGCAGCTGATGUCGCCGTACGGATCCACGT Fam

dRP Lyase Anti-sense 43-mer DNA

5’-ACGTGGATCCGTACGGCGGCATCAGCTGCAGGCATCTAGTCTA

Fen1 UPS Sense 24-mer DNA

5’-TAGACTAGATGCCTGCAGCTGATG

Fen1 DWS Sense 28-mer DNA

5’-Fam AAATTGGGTTCGCCGTACGGATCCACGT

UPS Sense Ligase1 25-mer

5’-Fam TAGACTAGATGCCTGCAGCTGATGC

DWS Sense Ligase1 18-mer

5’-phospho-CGCCGTACGGATCCACGT Fam

2.3.1. Synthesis and labeling of DNA substrates—To examine the effect of ISY1 on APE1’s 5’-endonuclease activity, a 63-mer oligonucleotide with and without the AP site analogue was synthesized and reconstituted in TE buffer as described earlier (38).This DNA was labeled with [$\gamma-^{32}$P]ATP at the 5′-end using T-4 polynucleotide kinase, and annealed to a complementary oligonucleotide strand using a standard protocol. The labeled oligomers were purified using Nick column as described by the manufacturer (GE Healthcare Biosciences, Pittsburgh, PA), quantitated and stored at −20°C.

2.3.2. Purification of APE1, ISY1, POL β, FEN1, LIG1, XRCC1/Ligase 3 and Metnase—

Purified Human POL ß was provided by Samuel Wilson's lab (NIEHS, Research Triangle Park, NC, USA). Purified XRCC1/DNA Ligase 3 complex was provided by Alan Tomkinson (University of New Mexico, Albuquerque, NM, USA). Human recombinant APE1 was purchased from New England Biolab (NEB, Ipswich, MA, USA) and human recombinant ISY1 protein was purchased from Abnova (Walnut, CA, USA). Hexahistidine-tagged FEN1 and LIG1 proteins were overexpressed in BL21 (DE3) pLysS cells and purified to homogeneity according to our published protocols (39), while Metnase protein was purified from HEK293 cells stably overexpressing wild-type Metnase protein using affinity chromatography as previously described (40).

2.4. Nuclease activity Assay of APE1, ISY1 and Metnase

Nuclease activity was carried out in a standard reaction mixture (25 μl) containing 30 mm HEPES, pH 7.5, 30 mM KCl, 8 mM $MgCl_2$, 2 mM DTT, 0.01% Nonidet P-40, 0.1 mg/ml bovine serum albumin, and varying concentrations of APE1 and ISY1 recombinant proteins. Optimal concentrations of proteins were used to find the optimal time for the effect of ISY1 on APE1's nuclease activity. A similar reaction was assembled for recombinant Metnase protein to determine the effect of ISY1 on its nuclease activity. The reaction was initiated by addition of ^{32}P-labeled 63-mer F-DNA substrate. The reaction mixtures were incubated at 37 °C for 30 min for the dose curve of ISY1 and the reaction was terminated by addition of stop buffer (0.4% (w/v) SDS, 5 mM EDTA, 1 μg of proteinase K). Reactions were also carried out varying the time of incubation and terminated in the same manner. The DNA was recovered by phenol/chloroform extraction and ethanol precipitation. Recovered DNA was washed with cold 70% ethanol and suspended in sample loading dye. DNA suspended in 10 μl of gel loading solution (90% formamide, 1 mM EDTA, 0.1% xylene cyanol, and 0.1% bromphenol blue) and heated at 85 °C for 5 min. Samples (4 μl) were loaded onto a 15% denaturing polyacrylamide and 7 M urea gel for electrophoresis. The gel was then dried under vacuum and dried gel was subjected to autoradiography to capture the radioactive signals.

2.4.1. dRP Lyase activity—

The reaction was assembled in 25 μl volume containing 30 mM Tris, pH 7.5, 30 mM KCl, 5 mM $MgCl_2$, 2 mM DTT, 0.01% Nonidet P-40, 1 mg/ml bovine serum albumin, UDG, APE1, POL β and varying concentrations of ISY1 recombinant proteins. The reaction was initiated by the addition of U-DNA substrate. Optimal concentrations of proteins were used to find the optimal time for the effect of ISY1 on POL β's lyase activity (39). Initially, reaction mixtures were incubated with UDG for 20 min followed by addition of APE1 to generate the dRP substrate for POL β at 37 °C for 20 min. Once the dRP substrate was ready, POL β and ISY1 were added to the reaction mixture and incubated for additional 30 min at 37° C. After completion, dRP reaction products were stabilized by the addition of cold 340 mM sodium borohydride and incubated on ice for 30 min. The DNA was recovered by phenol/chloroform extraction and ethanol precipitated at −80º C. DNA was recovered by centrifugation and resuspended in sample loading dye. dRP products were resolved on a 15% denaturing polyacrylamide and 7 M urea gel. DNA on the gel was visualized by scanning in Typhoon Trio Biomolecular Imager (GE Healthcare Bio-Science Corporation, Piscatway, NJ, USA), at excitation of 526 nm and emission at 488 nm.

Digital images were acquired and analyzed for the quantitation using ImageQuant TL (GE Healthcare Bio-Science Corporation, Piscatway, NJ, USA) software.

2.4.2. Fen1 activity assay—*In vitro* Fen1 activity was performed in a final volume of 25 μl as described earlier (41). Briefly, the reaction mixture contained 30 mM Tris, pH 7.5, 30 mM KCl, 8 mM MgCl2, 1 mM DTT, and indicated amounts of Fen1 recombinant protein. Reaction was initiated by addition of flap substrate for Fen1. Reaction mixture was incubated at 37°C for 45 min and terminated by addition of a stop solution containing 0.4% (w/v) SDS and 5 mM EDTA. DNA was recovered by phenol/chloroform/isoamyl alcohol (25:24:1, v/v) extraction followed by ethanol precipitation. The 10-nt DNA product generated from the Fen1 activity was separated on a 15% acrylamide-7 M urea gel and visualized by scanning on Typhoon Trio Biomolecular Imager (GE Healthcare Bio-Science Corporation, Piscatway, NJ, USA) at excitation of 526 nm and emission at 488 nm). The digital images were acquired and analyzed for the quantitation using ImageQuant TL (GE Healthcare Bio-Science Corporation, Piscatway, NJ, USA) software.

2.4.3. DNA Ligase 1 or XRCC1/Ligase 3 activity assay—Similar reactions were assembled as described above for recombinant DNA ligase 1 or XRCC1/DNA ligase 3 protein to determine the effect of ISY1 on the ligation activity. For the DNA ligase assay 0.5 mM ATP was included in the reaction mixture. The reaction was initiated by addition of FAM-labeled appropriate nicked substrate for ligation. The reaction was allowed to proceed at 37 °C for 60 min and terminated by addition of stop buffer. The DNA was recovered by phenol/chloroform extraction, ethanol precipitation at −80° C and washing with 70% cold ethanol. The recovered DNA was resuspended in sample loading dye (90% formamide, 1 mm EDTA, 0.1% xylene cyanol). Samples were heated at 85 °C for 5 min and cooled quickly on ice. Samples (4 μl) were loaded onto a denaturing 15% polyacrylamide and 7 M urea gel for electrophoresis for separation of ligated products. The gel was scanned in Typhoon Trio Biomolecular Imager (GE Healthcare, excitation at 526 nm and emission at 488 nm). The digital images were acquired and analyzed for the quantitation using ImageQuant TL (GE Healthcare Bio-Science Corporation, Piscatway, NJ, USA). software.

2.4.4. In vitro reconstitution of SP- and LP-BER assay—*In vitro* SP- and LP-BER assays took place as previously described (28,49–52). The reaction mixture for SP-BER was essentially the same as that for LP-BER except that FEN1 was omitted in SPBER. Briefly, LP-BER reaction mixture contained 30 mM HEPES, pH 7.5, 30 mM KCl, 8 mM $MgCl_2$, 1 mM dithiothreitol, 100 μg/ml bovine serum albumin, 0.01% Nonidet P-40, 0.5 mM ATP, and 10 μM each of dATP, dCTP, dGTP, dTTP in a final reaction volume of 30 μl. The LP-BER reaction mixture was assembled on ice by the addition of 100 fMol of ^{32}P-labeled 63-mer F-DNA substrate, 25 fMol of AP endonuclease 1 (APE1), 25 pMol of POL β, 100 fMol FEN1 and 100 pMol of DNA ligase 1 and then incubated on ice for 5 min. The reaction mixture was incubated for 60 min at 37°C. Afterward the reaction was terminated by the addition of stop buffer (0.4% (w/v) SDS, 5 mM EDTA, 1 μg of proteinase K) and incubated at 37 °C for an additional 30 min (19,38,39,42–44). The DNA was recovered by phenol/chloroform extraction and ethanol precipitation. Recovered DNA was washed with cold 70% ethanol and suspended in sample loading dye. The reaction products were separated on a 15%

acrylamide and 7 M urea gel. The gel was transferred to blotting sheet (3 mm Chromatographic paper, Whatman), dried and radioactive signals were visualized by autoradiography.

2.5. Electrophoretic Mobility Shift Assay (EMSA)

Before assembling the reaction, we ascertained the quality and quantity of recombinant proteins (Fig. 3S). There was no detectable APE1 in the purified ISY1. DNA-protein binding reactions were assembled in 20 μl of final volume, containing 20 mM HEPES, pH 7.9, 1 mM dithiothreitol, 3.5 mM $MgCl_2$, 100 mM KCl, 0.03% (v/v) Nonidet P-40, 10% (v/v) glycerol, 1 μg of poly (dI-dC), and varying amount of purified recombinant APE1 and ISY1 proteins. Recombinant human APE1 and ISY1 proteins were purchased from New England Biolabs (Ipswich, MA) and Abnova (Walnut, CA, USA), respectively. Reactions were initiated by the addition of 100 fMol of ^{32}P-labeled control and ^{32}P-37-mer F-DNA oligonucleotides (45–47). Reactions proceeded for 20 min at room temperature, and then the entire reaction mixture was loaded directly onto a native 5.5 % polyacrylamide gel. For competition experiments, a molar excess of unlabeled oligonucleotide was added to the reaction mixture 10 min prior to the addition of ^{32}P-labeled probe, as indicated in the figure legends. To further validate the specific binding to AP DNA, we used super-shift analysis. For super-shift analysis, 1 μg of anti-APE1 (Ab82, Abcam, Cambridge, MA, USA) was added to the reaction mixture and incubated for 20 min before the addition of ^{32}P-labeled oligonucleotide. The gel was run in the cold room (4° C) in 1x TBE buffer. After the completion of electrophoresis, the gel was transferred to a blotting sheet (3 mm Chromatographic paper, Whatman) and dried. DNA-protein complexes were visualized by autoradiography.

2.6. Immunoprecipitation and western analysis

Immunoprecipitation was used to test the protein:protein interaction between APE1 and ISY1. Briefly, HCT-116 or HCT116(APE1kd) cells (1×10^5) were collected, washed with cold PBS, and lysed in a buffer containing 25 mM Tris-HCl (pH 7.5), 0.3 mM NaCl, 1.5 mM $MgCl_2$, 0.2 mM EDTA, 0.5% Triton X-100, 10 mM β-glycerophosphate, 1 mM sodium vanadate, 1 mM DTT, protease inhibitor cocktails and 1 mM phenylmethylsulfonyl fluoride (Thermo-Fisher Scientific, Waltham, MA, USA). After lysis cell debris were removed by centrifugation at 20,000 × g at 4°C. Cell lysates were collected in a fresh tubes and protein quantitated using Bradford reagent (Bio-Rad, Hercules, CA, USA). Cell lysates were precleared with beads and precleared lysate was used for immunoprecipitation. Immunoprecipitation was performed with magnetic beads cross-linked with antibody using a IP/Co-IP kit, as described by the manufacturer (Thermo-Fisher Scientific, Waltham, MA, USA) (48). The immunocomplex was captured on protein A/G magnetic beads, washed with wash buffer (3× times) and suspended in loading sample buffer. Samples were denatured by boiling for 10 min and supernatant was loaded onto a SDS-PAGE gel and electrophoresed. Proteins were transferred to a PVDF membrane (Millipore, Billerica, MA), blocked with fat-free milk and immunoblotted with primary antibody followed by peroxidase-coupled secondary antibody (Amersham Biosciences, USA). Signal was detected by enhanced chemiluminescence (Thermo-Fisher Scientific, Waltham, MA) reaction prior to visualization on Kodak-X-Omat film.

2.6.1. In Vitro Immunoprecipitation—*In vitro* immunoprecipitation was carried out using Capturem IP kit from Takara (Takara, Mountainview, CA, USA). Immunoprecipitation was initiated by mixing of 1 μg of recombinant proteins with IgG control or ISY1 antibody in 150 μl of equilibration buffer at 4°C. The antibody complex was captured on the column and unbound proteins were washed using equilibration and wash buffer. Bound proteins were eluted using elution buffer and immediately neutralized with 1 M Tris pH 8.0. Samples were analyzed by western blot analysis.

2.7. Western blot analysis

Protein levels of ISY1, APE1, DNA POL β, FEN1, LIG1 and β-actin proteins were determined by western blot analysis with our previously described procedure (48,49). The antibodies for ISY1 and β-actin were purchased from Sigma (St Louis, MO, USA), FEN1, DNA ligase 1 were purchased from Novus Biologicals (Centennial, CO, USA) and APE1, POL β were purchased from Abcam (Cambridge, MA, USA), respectively.

2.8. Clonogenic Cell Survival assay

Clonal cell survival was determined by plating transfected cells (HCT-116 cells with or without ISY1) plated at a density of 5×10^2 cells per well in a 6-well plate in triplicate. After attachment cells were treated with different concentrations of H_2O_2 and MMS (methyl methanesulfonate) (Sigma, St. Louis, MO, USA) for 24 h. After this time, medium containing H_2O_2 or MMS was removed, cells were washed once in medium, and fresh medium was added. Cells were allowed to grow for 7–10 days to form the visible colonies. When colonies were visible (>50 cells), colonies were stained using methylene blue (38,50). Stained colonies were dried and counted using Image J (US National Institute of Health, Bethesda, MD, USA). The surviving fraction was calculated by normalizing against the colony numbers achieved for the untreated wells. Colonies containing less than twenty cells were excluded from the counting. Unpaired Student *t* tests were used for all statistical analysis, unless otherwise indicated.

2.9. Protein modelling

A model of human ISY1 was generated in SWISS-MODEL using the ISY1 component of the yeast spliceosome (PDB: 5LJ3) as a template (51). The crystal structure of human APE1 in complex with DNA was previously determined (PDB: 1DE9) (52). A plausible binding surface between APE1-DNA and lSY1 was predicted and modeled in the interactive modeling program Coot (53). The model showing interaction between DNA and protein was produced in PyMOL (54).

2.10. Statistical analysis

All experiments were repeated at least three-times and data were expressed as mean ± SE. Statistical analysis was performed using Two Way analysis of variance (ANOVA) by using SigmaPlot 13 (Systat Software, San Jose, CA). A one-tailed t-test was used to compare any significant difference between control and treated groups. The criterion for statistical significance was $p<0.05$. For western blotting data, band intensities were measured using Image J and normalized with the loading control (α-tubulin or β-actin) (55).

3. RESULTS

3.1. APE1 interacts with ISY1

First, we determined the expression levels of ISY1 and APE1 in a panel of untreated cell lines by western blot analysis. We found that both ISY1 and APE1 are abundantly present in all cell lines tested (Fig 1a). We also tested whether depletion of APE1 has any effect on the expression of ISY1 and vice-versa. We found that APE1 depletion does not affect the expression of ISY1 protein. These results suggest that APE1 does not regulate ISY1 gene expression (Fig. 1a, lanes 4 and 5; Fig. 1c, compare lanes 2 and 3). Likewise, depletion of ISY1 has little effect on APE1 levels (Fig. 1c). We also tested whether ISY1 depletion affects the expression of any other BER proteins. The results from western blot analysis indicated that the expression of the BER proteins, APE1, POL β, FEN1 and LIG1 is not affected by ISY1 depletion (Fig. 1c).

Next, we asked whether the DNA alkylating agent methyl methanesulfonate (MMS) has any effect on the expression of ISY1. MMS mono-alkylates guanines and adenines, resulting in mispairing during replication and point mutations. Most methylating agents form adducts at N- and O- atoms in DNA bases, each with distinct stabilities (56). Our results showed that expression of ISY1 protein is increased in both APE1 wild-type and APE1 depleted cells after MMS exposure, while APE1 protein levels remains unaffected (Fig. 1d). These results revealed that enhanced expression of ISY1 after DNA alkylation damage is independent of APE1 (Fig. 1d).

We further demonstrated that ISY1 interacts with APE1. We immunoprecipitated ISY1 from extracts of APE1 wild-type (WT) and APE1-depleted HCT116 cells. We found that ISY1 physically associates with APE1 (Fig. 1e, compare lanes 1 and 2 with 3 and 4). However, it is possible that this co-immunoprecipitation might occur because both proteins bind to DNA. We ruled out this possibility by treating the cell lysate with DNase I. Treatment with DNase I did not affect co-immunoprecipitation of APE1 proteins in wild-type and APE1-knockdown HCT116 cells. ***Panel e and f*** shows co-immunoprecipitation of ISY1 without and with DNase I treatment of cell lysates, respectively. ***Panel g*** shows the co-immunoprecipitation of APE1 in wild-type and APE1-knockdown HCT116 cell extracts to examine the interaction with ISY1. ***Panel's h-k*** shows the co-immunoprecipitation of ISY1 in wild-type and ISY1-knockdown HCT116 cell extracts to show the lack of interaction of ISY1 with POL β, FEN1, DNA ligase I and ISY1, respectively.

APE1 by anti-ISY1 antibody (Fig. 1f), indicating that complex formation between APE1 and ISY1 occurs without DNA being present. We detected the presence of APE1 in the ISY1 immunocomplex in wild-type APE1 cells but not in APE1-depleted cells, as expected (Fig. 1e and 1f; compare lane 2 and 4). Reverse coimmunoprecipitation using anti-APE1 antibody confirmed that APE1 and ISY1 interact with each other (Fig. 1g, compare lane 2 with 4). We also found that ISY1 does not interact with the BER proteins, POLβ, FEN1 or LIG1. Thus, ISY1 specifically interacts with APE1 (Fig. 1g–k).

However, it is possible that this co-immunoprecipitation might involve presence of RNA, since it has been shown that APE1 interaction with nucleophosmin (NPM1) requires RNA

(57), and that APE1 and ISY1 both interact with RNA. Therefore, we ruled out this possibility by treating the cell lysate with RNase A. Treatment with RNase A did not affect co-immunoprecipitation of APE1 by anti-ISY1 antibody (Fig. S1). We further validated this interaction using purified recombinant APE1 and ISY1 proteins. Our results demonstrate that ISY1 interacts with APE1 (Fig. S2).

3.2. ISY1 stimulates the endonuclease activity of APE1

Since ISY1 interacts with APE1, we asked whether ISY1 influences APE1's catalytic activity. We first tested the activity of ISY1 and APE1 on a ^{32}P-labeled 63-mer DNA substrate that contains a unique synthetic AP site. As expected, APE1 incised the substrate at the AP site to generate a 5'-labeled 23-mer product (Fig. 2b, compare lanes 4–8), while ISY1 had no such activity (Fig. 2b, lanes 1–3). We next tested the effect of ISY1 on AP site incision by a sub-optimal concentration of APE1 (Fig. 2b and 2c, lanes 1116). Importantly, the addition of an increasing amount of ISY1 greatly potentiated the activity APE1 (Fig. 2b, lanes 13–16), reaching nearly 100% cleavage upon addition of 10 ng (300 fmol) of ISY1 to a reaction containing 0.25 ng (7.5 fmol) APE1 (Fig. 2b, compare lanes 2, 4 and 14). Using the sub-optimal concentrations of APE1 activity in lane 4 and 5, we further assessed the stimulatory effect of ISY1 as a function of the reaction time (Fig. 2c, lanes 11–15). Our results suggest that ISY1 at sub-nanomolar concentrations can markedly promote APE1 endonuclease activity (Fig. 2c, lane 11–15).

3.3. Effect of ISY1 on other BER enzymes

We further examined whether ISY1 affects the activity of other BER proteins such as the dRP lyase activity of POL β, the flap endonuclease activity of FEN1 and the ligase activity of DNA Ligase1 and XRCC1/Ligase 3. We used appropriate DNA substrates as described earlier to demonstrate that ISY1 does not affect the activity of any other BER pathway enzymes such as dRP lyase activity of DNA polymerase β, Fen1 and DNA ligase 1 or XRCC1/DNA ligase 3 (Fig. 3a–e). We also tested whether time dependent incubation with ISY1 affects dRP lyase activity, flap endonuclease activity and DNA ligase activity. We found that ISY1 has no effect on the dRP lyase activity of POL β, flap-endonuclease activity of FEN1 and ligase activity of both DNA ligase1 and XRCC1/Ligase 3 (Fig. S3). Likewise, ISY1 did not affect the endonuclease activity of another DNA repair protein, Metnase (Supplemental Fig. S2 b and c, lanes 7–11). Based upon these results, we concluded that ISY1 specifically activates APE1 endonuclease activity.

3.4. ISY1 activation of APE1 facilitates SP-BER

We next examined whether ISY1 regulates APE1 endonuclease activity within the context of SP-BER. We used three different BER conditions to test the possible involvement of ISY1 in SP-BER. First, we used an optimal concentration of APE1 and validated the progress of SP-BER through to completion. We then used a suboptimal concentration of APE1 and followed the progress of SP-BER, demonstrating its failure. In the third condition, we used a sub-optimal concentration of APE1 combined with ISY1 and measured the completion of SP-BER. The omission of FEN1 prevented the occurrence of LP-BER.

We assembled the BER reaction as described in Figure 4a with a ^{32}P-labeled uracil-containing DNA substrate that had been pretreated with uracil-DNA glycosylase to generate an AP site at the 24th position from the ^{32}P-labeled DNA end. Following incision by APE1 which cleaved the phosphodiester backbone 5'-upstream of the AP site, thereby generating a 23-mer incised product (Fig. 4b, compare lane 1 with 4). Subsequent, addition of POL β, dNTPs, and LIG1 led to the production of the completely repaired ^{32}P-63-mer product (Fig. 4b, compare lanes 4, 5 and 7).

As expected, little repaired product was seen when we used a suboptimal amount of APE1 (0.25 fMoles) in the reconstituted reaction (Fig. 4b, compare lane 4 with 11 and 7 with 14). These results show that a sub-optimal concentration of APE1 was insufficient to drive this reaction to completion, indicating that APE1 activity is critical and requires optimal activity to fully achieve the completion of SP-BER.

Importantly, under these conditions of limited APE1 availability, the inclusion of ISY1 (400 fMoles) allowed BER to proceed to completion. We found that the presence of ISY1 activated APE1 and facilitated the completion of repair of the ^{32}P-U-DNA by SP-BER (Fig. 4b, compare lane 4 with 11, lane 11 with 22, and lane 14 with 25). These results revealed a stimulatory role of ISY1 in SP-BER via its influence on APE1 activity.

3.4. ISY1-mediated activation of APE1 facilitates LP-BER

To determine the effect of ISY1 on APE1-mediated LP-BER, we reconstituted LP-BER *in vitro* as outlined in Figure 4a. First, we validated our LP-BER *in vitro* reaction using optimal concentrations of APE1, POL β, FEN1 and LIG1. The results showed that, as expected, APE1 generated cleaved ^{32}P-labeled 23-mer products and 40-mer unlabeled products (Fig. 5b, compare lane 1 with 2) that could be extended by POL β to form a predominantly 24-mer product (Fig. 5b, compare lane 2 and 3). After further addition of FEN1, we saw the appearance of DNA synthesis products of 2–7 nt, indicating that FEN1 enhanced DNA strand-displacement synthesis by POL β (Fig. 5b, compare lanes 3 and 5). The addition of LIG1 sealed the nick and re-generated the completely repaired ^{32}P-labeled 63 nt product. The appearance of the ligated full length 63 nt product was consistent with FEN1-mediated removal of the DNA flap created by strand displacement synthesis.

When we used a sub-optimal concentration of APE1 in this assay system, no APE1-mediated nicking of the ^{32}P-63-mer F-DNA substrate was detected (Fig. 5b, compare lanes 2 and 9). Addition of POL β (Fig. 5b, compare lanes 2 and 3 with 9 and 10, respectively), FEN1 and DNA ligase I (Fig. 5b, compare lanes 7 and 14) did not permit completion of LP-BER when using sub-optimal concentration of APE1. It appears that Fen1 or LIG1 also stimulates endonuclease activity of APE1 when limiting concentrations of APE1 were present. APE1 after cleaving the abasic DNA might facilitates the binding and synthesis of the strand displacement products by the presence of DNA polymerase β, FEN1, and DNA ligase I. This may imply that BER can be differentially regulated. However, assembly of relevant constituent proteins of BER pathway may affect the overall BER pathway.

We next proceeded to determine whether the inclusion of ISY1 would enable BER with the use of the sub-optimal APE1 amount. Importantly, the results showed increased APE1

activity upon addition of ISY1 (0.5 pmol) (Fig. 5b, compare lanes 9 and 10 with 17 and 19, respectively), and the further addition of POL β, FEN1, and LIG1 allowed the repair reaction to go to completion (Fig. 5b, lane 24). Thus, ISY1 enhances the activity of APE1 and also the efficiency of LP-BER.

3.5. ISY1 promotes APE1 binding to AP sites in DNA

Our results above have provided evidence for a role of ISY1 in activating the endonuclease activity of APE1 to facilitate both SP- and LP-BER. We next examined whether ISY1 affects the binding of APE1 to AP site DNA by the electrophoretic mobility gel-shift assays (EMSA). We assembled the reaction with ^{32}P-labelled duplex DNA that harbors an AP site (F-DNA) or a control duplex which did not. The results showed that APE1 has a much higher affinity for the F-DNA compared to the control DNA (Fig. 6a, compare lanes 2–4 with 8–10). The control DNA without an AP-site did not bind to APE1. The specificity of F-DNA binding to APE1 was further confirmed by the addition of APE1 antibody to the reaction mixture. This led to the supershifting of the F-DNA:APE1 nucleoprotein complex (Fig. 6b, compare lane 2, 3 and 4). ISY1 did not interact with the ^{32}P-Control DNA but it did have slight binding to the ^{32}P-F-DNA (Fig. 6a, compare lanes 5–7 with 11–13).

Next, we determined the effect of ISY1 on APE1 binding to AP site DNA. Increasing concentrations of ISY1 enhanced binding of APE1 to ^{32}P-F-DNA in the presence of ISY1 (Fig. 6c, compare lane 2–4 with lane 8–10, respectively). We tested increasing concentrations of ISY1 in EMSA, and found that increasing concentrations did slightly enhance ISY1 binding to ^{32}P-F-DNA. Importantly, the ability of APE1 to bind ^{32}P-F-DNA was enhanced 4-fold by increasing amounts of ISY1 (Fig. 6c and 6d, compare lanes 2–4 with lanes 8–10 and with lanes 11–13).

3.6. ISY1 enhances cell survival after exposure to DNA alkylation damage or oxidative stress

We performed clonogenic cell survival assays to ascertain whether ISY1 is needed for cellular resistance to DNA damage caused by monofunctional DNA alkylating agents or oxidative stressors that is predominantly repaired via BER (58). We hypothesize that cells lacking ISY1 will be more sensitive to DNA damaging agents that are repaired via the BER pathway. Treatment with MMS results in the mono-methylation of guanine and adenine to yield 7-methylguanine and 3-methyladenine, either of which can interfere with DNA replication. These lesions are removed by LP-BER (38). We examined the clonogenicity of control or ISY1-depleted HCT-116 cells treated with different concentrations of MMS. We found that depletion of ISY1 alone, reduced the plating efficiency to 9.2% compared to scrambled siRNA control of 17.2%, suggesting that ISY1 plays role in normal cell function, either via splicing or in repair of oxidized DNA (Fig. 7A). When ISY1-depleted cells were stressed with MMS and survival was normalized to ISY1 depletion alone, the ISY1 cells had a further 2.1-fold decrease in survival compared to scrambled siRNA control cells at 125 μM of MMS (Fig. 7A). Likewise, HCT-116 cells depleted of ISY1 and stressed with H2O2 had a further 3.1-fold decrease in clonogenicity compared to scrambled control cells at 15 μM H2O2 (Fig. 7B). From these results, we conclude that ISY1 is important for cell survival in the presence of DNA alkylation or oxidative stress.

3.7. DNA alkylation and oxidative stress-induced damage effects are rescued by APE1 expression in ISY1 knock-down cells

MMS, an alkylating agent that introduces base modifications in DNA and promote AP site production via direct (increased hydrolysis) and indirect (DNA glycosylase excision) mechanisms (59,60). If these AP sites are not repaired in a timely fashion, they eventually become single-strand break.

We reasoned that if ISY1 repression creates a deficiency in repair of single strand break then APE1 - overexpression could compensate for this deficiency of ISY1. We measured the repair capacity of cells by measuring the reversal of toxicity of MMS or H2O2 after APE1 overexpression. We treated ISY1 knock-down cells and APE1 overexpressed cells with H2O2 (5–10 μM) and MMS (75–100 μM) for 24h and then allowed the cells to grow in DNA alkylating and oxidative stressor free medium. This will provide cells an opportunity to repair the damaged DNA as result of these insults. We quantitated the cells which survived DNA alkylation and oxidative stress-induced damage. Survival data showed that APE1 overexpression (Flag-hAPE1) did indeed rescue the H2O2 or MMS-induced toxicity in ISY1 knock-down cells (Fig. 8, panel a-d; compare ISY1 knock-down group with ISY1+APE1 overexpressed group, compare lane 1–3 with 4–6; *panel* b and d). APE1 overexpression provided cells an advantage for the colony survival by about 20%. This gain of survival of 20% was observed in both MMS and H2O2 treatment. These results demonstrate that repair capacity of APE1 overexpressed cells were significantly increased as compared to ISY1 repressed cells (Fig. 8a–d, compare ISY1 group with ISY1+APE over expressed group).

3.8. Modeling of the interaction of ISY1 with APE1

To define a molecular mechanism by which ISY1 might enhance APE1 AP-DNA binding, three different crystal structures of DNA-free human APE1 with Mg^{2+} as a cofactor and three co-crystal structures of human APE1 bound to AP-DNA were analyzed. These crystal structures indicate that APE1 uses a rigid, pre-formed, positively charged surface to kink the DNA helix and engulf the AP-DNA strand. APE1 inserts active site loops into both the DNA major and minor grooves and binds to a flipped-out AP site in a pocket that excludes DNA bases (52). We virtually analyzed the potential for ISY1 to enhance APE1 binding to AP-site DNA using these crystal structures. Our analysis concluded that N-terminal ISY1 interaction with the APE1:AP DNA complex had a decreased energy state compared to APE1:AP-DNA alone (Fig 8). Our modeling predicts that ISY1 binding to APE1:AP-DNA would alter its three-dimensional configuration, and slightly open the APE1 catalytic site. The N-terminal region of ISY1 also appears to secure the APDNA into place in the APE1 active site. This would explain the increased binding of APE1 to AP-DNA when ISY1 is present.

APE1 and ISY1 were predicted to form a four-helix bundle interface with a surface area of approximately 1500 Å, indicating a strong binding interaction. In addition, many of the predicted interactions occur between polar residues and are likely to be involved in hydrogen bonding. The N-terminal aa 1–17 of ISY1 is predicted to form two short helices that orient into the major groove of the DNA, locking the AP region of the DNA into the widened active site of APE1. This results in a more stable APE1:AP-DNA complex (Fig. 8).

4. DISCUSSION

Oxidative and alkylating insults generate DNA base lesions and AP sites which are eliminated by BER. If these lesions are not adequately repaired, they that can impede both transcription and replication, resulting in cell death or neoplastic transformation. BER is the principal mechanism for the removal of these base lesions. In this report, we describe the finding that the splicing factor ISY1 interacts with APE1, promotes its specific binding to abasic DNA, and enhances its endonuclease activity, thereby promoting both SP- and LP-BER. While in most circumstances APE1 levels are not limiting normally, there are cellular environments where BER is limited by low levels of APE1. For example, overwhelming oxidative stress results in p53 activation, and activated p53 can decrease APE1 gene expression (61,62). This could occur as part of the apoptotic process, to prevent genomic repair to promote cell suicide (61–63). Since ISY1 expression is induced by base damaging agents it could serve as a secondary regulator of BER, promoting it when it is required, and then fading back to baseline after the threat has been eliminated. ISY1 could be part of a final cellular defense against oxidative DNA damage before apoptosis.

This raises the question of why a secondary regulator for APE1 is needed in BER, and why not just have continuously high levels of APE1. A potential rationale for such a secondary regulator is that when high levels of APE1 are mismatched with lower levels of later BER components, there would be an increase in unrepaired DNA SSBs stemming from the incision of AP sites. When encountered by a replication fork, these SSBs are converted into DSBs, which could lead to genomic instability (10–14, 46, 47). Thus, constant APE1 levels with temporal increases in its activity by induction of ISY1 or decreasing its expression with induction of p53 would permit precise regulation of APE1 activity without mismatching its steady state expression levels with later BER components.

There is a second reason why ISY1 regulation of APE1 could be important in normal cell function. APE1 levels are often decreased in aging tissues, which would lead to oxidative genomic damage that would accelerate the aging process (63–66). For example, APE1 expression becomes diminished in aging motor neurons, marrow mesenchymal stem cells and hepatocytes. These cells lose expression of APE1 and accumulate oxidative genomic damage (63–66). Also, it has been observed that base excision repair activity in germ cells declines with the age, which was reversed by the addition of APE1 (67). As such, ISY1 could be an anti-aging factor, preventing this accumulation of oxidative genomic damage by enhancing the activity of the remaining APE1. Tissue aging would become irreversible only when ISY1 expression is also impaired (65,66). Failure of ISY1 to be induced by DNA base damage could be a biomarker of aging. Enhancing ISY1 expression or activity could potentially prevent oxidative damage in aging organs and preserve their function for longer time periods. Thus, ISY1 not only ensures the accuracy of splicing, it ensures the accuracy of the DNA template from which the pre-mRNA is transcribed.

In general, high expression of APE1 is a hallmark of neoplasia, and the higher the level, the worse the prognosis for a given cancer (68,69). Higher levels of APE1 promote tumor survival by ameliorating the negative effects of enhanced oxidative stress encountered in transformed cells (70). In hepatocellular carcinoma, APE1 expression is up-regulated from

increased transcription because of the heightened oxidative status of the transformed cells (70). One would hypothesize that most cancers would require higher APE1, yet that is not observed (37,38). One possibility for malignancies to overcome the oxidative stress of oncogenic transformation would be ISY1. Higher levels of ISY1 could promote the activity of APE1 to repair the oxidative insults that arise from the changes in metabolism during neoplastic transformation (68,70), reducing the need for increased levels of APE1.

Neoplastic cells could also subvert ISY1 to resist monofunctional alkylating chemotherapy. Enhanced induction of ISY1 during alkylator therapy could increase the survival of cancer cells during chemotherapy. Thus, ISY1 levels post-chemotherapy could be a prognostic marker of resistance. In addition, targeting ISY1 with a small molecule might result in increased response to alkylating chemotherapy. There is precedent for this possibility; the homeobox protein CUX1 enhances the activity of APE1 in BER and thereby promotes the resistance to chemotherapy in glioblastoma cells (71).

Recently, there are other several reports consistent with the hypothesis that splicing factors can promote DNA repair and genomic stability. For example, splicing components can bind to nascent transcripts and prevent genomic instability by deterring the formation of R-loops (72). PSO4/PRP19, an essential pre-mRNA splicing component, is strongly upregulated by DNA damage in human cells (40,73). The pre-mRNA splicing complex in which PSO4 resides also contains XAB2, SEV, CDC5L, PLRGl, and Spf27. PSO4 also colocalizes with Metnase at DSBs induced by ionizing radiation (40). PSO4 enhances the endonuclease activity of Metnase (74), similar to the function of ISY1 described here. Depletion of PSO4 by siRNA results in an accumulation of DSBs, apoptosis and reduced survival of cells after exposure to ionization radiation (40,75). XAB2 and PSO4 have been reported to enhance DNA end resection and ATR activation during homologous recombination (76,77). In addition, the alternative splicing factor/splicing factor 2 (ASF/SF2) binds to PARP1, a component of both SSB repair and BER (78). These studies have thus established a link between splicing and DNA repair. Based upon our results we predict that pre-mRNA splicing and DNA repair share a component APE1. Both processes have to accurately recognize specific differences in nucleic acid sequences, and/or subtle changes in the chemistry of the bases. Sharing components would be much more efficient from an evolutionary standpoint (79,80).

We propose that the N-terminal domain of ISY1 interacts with the catalytic domain of APE1 and is involved in enhancing its abasic site binding and nuclease activities. Future studies will determine precise domains and their amino acids involved in the interaction of ISY1 and APE1. Our modeling predicts that APE1 changes its three-dimensional configuration after ISY1 binding, exposing the APE1 catalytic site. This more open structure of the APE1 catalytic site would promote APE1 AP-DNA binding, and thereby enhance its endonuclease activity, consistent with a model proposed in previous studies (52). The ISY1 N-terminal region also folds over the AP-DNA site in APE1 and appears to stabilize the AP-DNA in the active site. Our virtual model not only predicts that ISY1 would enhance the binding AP-DNA to APE1, but that it could also directly enhance its nucleolytic activity by opening the catalytic site. The ISY1 N-terminal positively charged amino acids could promote the cleavage 5’ of the AP site by hydrogen bonding with the phosphodiester linkages on the

damaged strand, resulting in a lower energy not only for AP-DNA binding but also for activation of cleavage. Thus, genomic instability could play a role in diseases caused by dysregulation of splicing factors, such as myelodysplastic syndrome and acute leukemia, retinitis pigmentosa, cystic fibrosis and spinal muscular atrophy.

5. Conclusion

Splicing factor ISY1 interacts with APE1 and enhances binding of APE1 to abasic DNA lesions. It also promotes APE1-mediated 5'−3' endonucleolytic cleavage of an abasic site. We also observed that ISY1 expression is induced by mono-alkylating DNA damage which is repaired by BER. These studies have a biological significance in aging tissues where loss of APE1 expression could result in accumulation of abasic lesions as a result of endogenous oxidative stress. Under these circumstances, ISY1 expression could compensate for the reduced level of APE1 by enhancing its catalytic activity and prevent the oxidative DNA damage. Additionally, the cross-talk of splicing with BER provides a basis for the genomic instability seen in diseases caused by mutations in splicing components, such as in myelodysplasia and acute leukemia. This study demonstrates that splicing and base excision repair (BER) share a common component ISY1, which catalyzes the rate-limiting step of BER.

Supplementary Material

Refer to Web version on PubMed Central for supplementary material.

Acknowledgements:

We are grateful to the following investigators for generous gift of the reagents: Dr. Samuel H. Wilson and Dr. Rajendra Prasad (Laboratory of Structural Biology, NIEHS, NIH, Research Triangle Park, NC) for providing purified human POL ß and anti-POL ß antibody. Dr Alan Tomkinson, (Department of Internal Medicine, The University of New Mexico) for providing XRCC1/DNA ligase 3 complex. Dr. Tomas Lindahl (Cancer Research U.K. London Research Institute, Clare Hall Laboratories, South Mimms, Hertfordshire, U.K.) for human DNA ligase I, and Dr. Ulrich Hubscher (Institut fur Veterinarbiochemie, Universitat Zurich-Irchel, Winterthurerstrasse, Zurich, Switzerland) for the human FEN1 overexpression plasmid. We are also thankful to Dr Tadahide Izumi for providing us APE1 stable knock-down cells (College of Medicine, University of Kentucky, KY). We thank Dr Kishore Bhakat (Department of Genetics, University of Nebraska Medical Center) for Flag-APE1 wt plasmid.

Footnote: This study was supported by grants from the National Institutes of Health (NIH) R01 CA139429 and R01 GM109645 to RH, and R01 CA220123 to PS.

Abbreviations:

APE1	apurinic/apyrimidinic endonuclease1
BER	Base excision repair
EMSA	electrophoretic mobility shift assay
FEN1	flap endonuclease1
PAGE	polyacrylamide gel electrophoresis
POL β	DNA polymerase β

RON	reactive nitrogen species
ROS	reactive oxygen species
SiRNA	small-interfering ribonucleic acid
SSB	single strand-break
UDG	uracil DNA glycosylase

REFERENCES:

1. Hoejmakers JH (2001) Genome maintenance mechanisms for preventing cancer. Nature 411, 366–374 [PubMed: 11357144]
2. Lindahl T (1993) Instability and decay of the primary structure of DNA. Nature 362, 709–715 [PubMed: 8469282]
3. Kidane D, Murphy DL, and Sweasy JB (2014) Accumulation of abasic sites induces genomic instability in normal human gastric epithelial cells during Helicobacter pylori infection. Oncogenesis 3
4. Cerutti PA (1994) Oxy-radicals and cancer. Lancet 344, 862–863 [PubMed: 7916406]
5. Kidane D, Chae WJ, Czochor J, Eckert KA, Glazer PM, Bothwell ALM, and Sweasy JB (2014) Interplay between DNA repair and inflammation, and the link to cancer. Crit Rev Biochem Mol 49, 116–139
6. Sancar A, Lindsey-Boltz LA, Unsal-Kacmaz K, and Linn S (2004) Molecular mechanisms of mammalian DNA repair and the DNA damage checkpoints. Annu Rev Biochem 73, 39–85 [PubMed: 15189136]
7. Wilson DM 3rd, Bohr VA, and McKinnon PJ (2008) DNA damage, DNA repair, ageing and age-related disease. Mech Ageing Dev 129, 349–352 [PubMed: 18420253]
8. Wallace SS (2014) Base excision repair: a critical player in many games. DNA Repair (Amst) 19, 14–26 [PubMed: 24780558]
9. Beard WA, Horton JK, Prasad R, and Wilson SH (2019) Eukaryotic Base Excision Repair: New Approaches Shine Light on Mechanism. Annu Rev Biochem 88, 137–162 [PubMed: 31220977]
10. Piersen CE, Prasad R, Wilson SH, and Lloyd RS (1996) Evidence for an imino intermediate in the DNA POLymerase beta deoxyribose phosphate excision reaction. J Biol Chem 271, 17811–17815 [PubMed: 8663612]
11. Yonekura S, Nakamura N, Yonei S, and Zhang-Akiyama QM (2009) Generation, biological consequences and repair mechanisms of cytosine deamination in DNA. J Radiat Res 50, 19–26 [PubMed: 18987436]
12. Evans AR, Limp-Foster M, and Kelley MR (2000) Going APE over ref-1. Mutat Res 461, 83–108 [PubMed: 11018583]
13. Li M, and Wilson DM 3rd. (2014) Human apurinic/apyrimidinic endonuclease 1. Antioxid Redox Signal 20, 678–707 [PubMed: 23834463]
14. Kelley MR, Georgiadis MM, and Fishel ML (2012) APE1/Ref-1 role in redox signaling: translational applications of targeting the redox function of the DNA repair/redox protein APE1/Ref-1. Curr Mol Pharmacol 5, 36–53 [PubMed: 22122463]
15. Mitra S, Boldogh I, Izumi T, and Hazra TK (2001) Complexities of the DNA base excision repair pathway for repair of oxidative DNA damage. Environ Mol Mutagen 38, 180–190 [PubMed: 11746753]
16. Scott TL, Rangaswamy S, Wicker CA, and Izumi T (2014) Repair of oxidative DNA damage and cancer: recent progress in DNA base excision repair. Antioxid Redox Signal 20, 708–726 [PubMed: 23901781]
17. David SS, O'Shea VL, and Kundu S (2007) Base-excision repair of oxidative DNA damage. Nature 447, 941–950 [PubMed: 17581577]

18. Kumar A, Abbotts J, Karawya EM, and Wilson SH (1990) Identification and properties of the catalytic domain of mammalian DNA polymerase beta. Biochemistry 29, 7156–7159 [PubMed: 2207097]

19. Caglayan M, Batra VK, Sassa A, Prasad R, and Wilson SH (2014) Role of polymerase beta in complementing aprataxin deficiency during abasic-site base excision repair. Nat Struct Mol Biol 21, 497–499 [PubMed: 24777061]

20. Cannan WJ, Rashid I, Tomkinson AE, Wallace SS, and Pederson DS (2017) The Human Ligase IIIalpha-XRCC1 Protein Complex Performs DNA Nick Repair after Transient Unwrapping of Nucleosomal DNA. J Biol Chem 292, 5227–5238 [PubMed: 28184006]

21. Mutamba JT, Svilar D, Prasongtanakij S, Wang XH, Lin YC, Dedon PC, Sobol RW, and Engelward BP (2011) XRCC1 and base excision repair balance in response to nitric oxide. DNA Repair (Amst) 10, 1282–1293 [PubMed: 22041025]

22. Caldecott KW (2003) XRCC1 and DNA strand break repair. DNA Repair (Amst) 2, 955–969 [PubMed: 12967653]

23. Gao Y, Katyal S, Lee Y, Zhao J, Rehg JE, Russell HR, and McKinnon PJ (2011) DNA ligase III is critical for mtDNA integrity but not Xrcc1-mediated nuclear DNA repair. Nature 471, 240–244 [PubMed: 21390131]

24. Simsek D, Furda A, Gao Y, Artus J, Brunet E, Hadjantonakis AK, Van Houten B, Shuman S, McKinnon PJ, and Jasin M (2011) Crucial role for DNA ligase III in mitochondria but not in Xrcc1-dependent repair. Nature 471, 245–248 [PubMed: 21390132]

25. Stucki M, Pascucci B, Parlanti E, Fortini P, Wilson SH, Hubscher U, and Dogliotti E (1998) Mammalian base excision repair by DNA polymerases delta and epsilon. Oncogene 17, 835–843 [PubMed: 9780000]

26. Fortini P, Pascucci B, Parlanti E, Sobol RW, Wilson SH, and Dogliotti E (1998) Different DNA polymerases are involved in the short- and long-patch base excision repair in mammalian cells. Biochemistry 37, 3575–3580 [PubMed: 9530283]

27. Braithwaite EK, Prasad R, Shock DD, Hou EW, Beard WA, and Wilson SH (2005) DNA polymerase lambda mediates a back-up base excision repair activity in extracts of mouse embryonic fibroblasts. J Biol Chem 280, 18469–18475 [PubMed: 15749700]

28. Fu D, Calvo JA, and Samson LD (2012) Balancing repair and tolerance of DNA damage caused by alkylating agents. Nat Rev Cancer 12, 104–120 [PubMed: 22237395]

29. Chanarat S, and Strasser K (2013) Splicing and beyond: the many faces of the Prp19 complex. Biochim Biophys Acta 1833, 2126–2134 [PubMed: 23742842]

30. Dix I, Russell C, Yehuda SB, Kupiec M, and Beggs JD (1999) The identification and characterization of a novel splicing protein, Isy1p, of Saccharomyces cerevisiae. RNA 5, 360–368 [PubMed: 10094305]

31. Fica SM, Tuttle N, Novak T, Li NS, Lu J, Koodathingal P, Dai Q, Staley JP, and Piccirilli JA (2013) RNA catalyses nuclear pre-mRNA splicing. Nature 503, 229234

32. Jurica MS, and Moore MJ (2003) Pre-mRNA splicing: awash in a sea of proteins. Mol Cell 12, 5–14 [PubMed: 12887888]

33. Hartmuth K, Urlaub H, Vornlocher HP, Will CL, Gentzel M, Wilm M, and Luhrmann R (2002) Protein composition of human prespliceosomes isolated by a tobramycin affinity-selection method. Proc Natl Acad Sci U S A 99, 16719–16724 [PubMed: 12477934]

34. Neubauer G, King A, Rappsilber J, Calvio C, Watson M, Ajuh P, Sleeman J, Lamond A, and Mann M (1998) Mass spectrometry and EST-database searching allows characterization of the multi-protein spliceosome complex. Nat Genet 20, 46–50 [PubMed: 9731529]

35. Agafonov DE, Deckert J, Wolf E, Odenwalder P, Bessonov S, Will CL, Urlaub H, and Luhrmann R (2011) Semiquantitative proteomic analysis of the human spliceosome via a novel two-dimensional gel electrophoresis method. Mol Cell Biol 31, 2667–2682 [PubMed: 21536652]

36. Staley JP, and Guthrie C (1998) Mechanical devices of the spliceosome: motors, clocks, springs, and things. Cell 92, 315–326 [PubMed: 9476892]

37. Matsuoka S, Ballif BA, Smogorzewska A, McDonald ER 3rd, Hurov KE, Luo J, Bakalarski CE, Zhao Z, Solimini N, Lerenthal Y, Shiloh Y, Gygi SP, and Elledge SJ (2007) ATM and ATR

substrate analysis reveals extensive protein networks responsive to DNA damage. Science 316, 1160–1166 [PubMed: 17525332]

38. Narayan S, Jaiswal AS, and Balusu R (2005) Tumor suppressor APC blocks DNA polymerase beta-dependent strand displacement synthesis during long patch but not short patch base excision repair and increases sensitivity to methylmethane sulfonate. J Biol Chem 280, 6942–6949 [PubMed: 15548520]
39. Balusu R, Jaiswal AS, Armas ML, Kundu CN, Bloom LB, and Narayan S (2007) Structure/function analysis of the interaction of adenomatous polyposis coli with DNA POLymerase beta and its implications for base excision repair. Biochemistry 46, 13961–13974 [PubMed: 17999539]
40. Beck BD, Park SJ, Lee YJ, Roman Y, Hromas RA, and Lee SH (2008) Human Pso4 is a metnase (SETMAR)-binding partner that regulates metnase function in DNA repair. J Biol Chem 283, 9023–9030 [PubMed: 18263876]
41. Jaiswal AS, and Narayan S (2008) A novel function of adenomatous polyposis coli (APC) in regulating DNA repair. Cancer Lett 271, 272–280 [PubMed: 18662849]
42. Jaiswal AS, Banerjee S, Panda H, Bulkin CD, Izumi T, Sarkar FH, Ostrov DA, and Narayan S (2009) A novel inhibitor of DNA polymerase beta enhances the ability of temozolomide to impair the growth of colon cancer cells. Molecular cancer research : MCR 7, 1973–1983 [PubMed: 19996303]
43. Jaiswal AS, Banerjee S, Aneja R, Sarkar FH, Ostrov DA, and Narayan S (2011) DNA polymerase beta as a novel target for chemotherapeutic intervention of colorectal cancer. PLoS One 6, e16691
44. Jaiswal AS, Balusu R, Armas ML, Kundu CN, and Narayan S (2006) Mechanism of adenomatous polyposis coli (APC)-mediated blockage of long-patch base excision repair. Biochemistry 45, 15903–15914 [PubMed: 17176113]
45. Masuda Y, Bennett RA, and Demple B (1998) Dynamics of the interaction of human apurinic endonuclease (Ape1) with its substrate and product. J Biol Chem 273, 30352–30359 [PubMed: 9804798]
46. Kim WC, Berquist BR, Chohan M, Uy C, Wilson DM 3rd, and Lee CH (2011) Characterization of the endoribonuclease active site of human apurinic/apyrimidinic endonuclease 1. J Mol Biol 411, 960–971 [PubMed: 21762700]
47. Jaiswal AS, and Narayan S (2001) p53-dependent transcriptional regulation of the APC promoter in colon cancer cells treated with DNA alkylating agents. J Biol Chem 276, 18193–18199 [PubMed: 11279192]
48. Kim HS, Nickoloff JA, Wu Y, Williamson EA, Sidhu GS, Reinert BL, Jaiswal AS, Srinivasan G, Patel B, Kong K, Burma S, Lee SH, and Hromas RA (2017) Endonuclease EEPD1 Is a Gatekeeper for Repair of Stressed Replication Forks. J Biol Chem 292, 2795–2804 [PubMed: 28049724]
49. Narayan S, Jaiswal AS, Sharma R, Nawab A, Duckworth LV, Law BK, Zajac-Kaye M, George TJ, Sharma J, Sharma AK, and Hromas RA (2017) NSC30049 inhibits Chk1 pathway in 5-FU-resistant CRC bulk and stem cell populations. Oncotarget 8, 57246–57264 [PubMed: 28915668]
50. Wu Y, Lee SH, Williamson EA, Reinert BL, Cho JH, Xia F, Jaiswal AS, Srinivasan G, Patel B, Brantley A, Zhou D, Shao L, Pathak R, Hauer-Jensen M, Singh S, Kong K, Wu X, Kim HS, Beissbarth T, Gaedcke J, Burma S, Nickoloff JA, and Hromas RA (2015) EEPD1 Rescues Stressed Replication Forks and Maintains Genome Stability by Promoting End Resection and Homologous Recombination Repair. PLoS Genet 11, e1005675
51. Arnold K, Bordoli L, Kopp J, and Schwede T (2006) The SWISS-MODEL workspace: a web-based environment for protein structure homology modelling. Bioinformatics 22, 195–201 [PubMed: 16301204]
52. Mol CD, Izumi T, Mitra S, and Tainer JA (2000) DNA-bound structures and mutants reveal abasic DNA binding by APE1 and DNA repair coordination [corrected]. Nature 403, 451–456 [PubMed: 10667800]
53. Emsley P, and Cowtan K (2004) Coot: model-building tools for molecular graphics. Acta Crystallogr D Biol Crystallogr 60, 2126–2132 [PubMed: 15572765]
54. Alexander N, Woetzel N, and Meiler J (2011) bcl::Cluster : A method for clustering biological molecules coupled with visualization in the Pymol Molecular Graphics System. IEEE Int Conf Comput Adv Bio Med Sci 2011, 13–18

55. Schneider CA, Rasband WS, and Eliceiri KW (2012) NIH Image to ImageJ: 25 years of image analysis. Nat Methods 9, 671–675 [PubMed: 22930834]
56. Brink A, Schulz B, Stopper H, and Lutz WK (2007) Biological significance of DNA adducts investigated by simultaneous analysis of different endpoints of genotoxicity in L5178Y mouse lymphoma cells treated with methyl methanesulfonate. Mutat Res 625, 94101
57. Vascotto C, Fantini D, Romanello M, Cesaratto L, Deganuto M, Leonardi A, Radicella JP, Kelley MR, D'Ambrosio C, Scaloni A, Quadrifoglio F, and Tell G (2009) APE1/Ref-1 interacts with NPM1 within nucleoli and plays a role in the rRNA quality control process. Mol Cell Biol 29, 1834–1854 [PubMed: 19188445]
58. Lindahl T, and Wood RD (1999) Quality control by DNA repair. Science 286, 1897–1905 [PubMed: 10583946]
59. Sedgwick B (2004) Repairing DNA-methylation damage. Nat Rev Mol Cell Biol 5, 148–157 [PubMed: 15040447]
60. Barnes DE, and Lindahl T (2004) Repair and genetic consequences of endogenous DNA base damage in mammalian cells. Annu Rev Genet 38, 445–476 [PubMed: 15568983]
61. poletto M, Legrand AJ, Fletcher SC, and Dianov GL (2016) p53 coordinates base excision repair to prevent genomic instability. Nucleic Acids Res 44, 3165–3175 [PubMed: 26773055]
62. Zaky A, Busso C, Izumi T, Chattopadhyay R, Bassiouny A, Mitra S, and Bhakat KK (2008) Regulation of the human AP-endonuclease (APE1/Ref-1) expression by the tumor suppressor p53 in response to DNA damage. Nucleic Acids Res 36, 1555–1566 [PubMed: 18208837]
63. Chu TH, Guo A, and Wu W (2014) Down-regulation of apurinic/apyrimidinic endonuclease 1 (APE1) in spinal motor neurones under oxidative stress. Neuropathol Appl Neurobiol 40, 435–451 [PubMed: 23808792]
64. Li M, Yang X, Lu X, Dai N, Zhang S, Cheng Y, Zhang L, Yang Y, Liu Y, Yang Z, Wang D, and Wilson DM 3rd. (2018) APE1 deficiency promotes cellular senescence and premature aging features. Nucleic Acids Res 46, 5664–5677 [PubMed: 29750271]
65. Luceri C, Bigagli E, Femia AP, Caderni G, Giovannelli L, and Lodovici M (2018) Aging related changes in circulating reactive oxygen species (ROS) and protein carbonyls are indicative of liver oxidative injury. Toxicol Rep 5, 141–145 [PubMed: 29854585]
66. Heo JY, Jing K, Song KS, Seo KS, Park JH, Kim JS, Jung YJ, Hur GM, Jo DY, Kweon GR, Yoon WH, Lim K, Hwang BD, Jeon BH, and Park JI (2009) Downregulation of APE1/Ref-1 is involved in the senescence of mesenchymal stem cells. Stem Cells 27, 1455–1462 [PubMed: 19492297]
67. Intano GW, McMahan CA, McCarrey JR, Walter RB, McKenna AE, Matsumoto Y, MacInnes MA, Chen DJ, and Walter CA (2002) Base excision repair is limited by different proteins in male germ cell nuclear extracts prepared from young and old mice. Mol Cell Biol 22, 2410–2418 [PubMed: 11884623]
68. Yuan CL, He F, Ye JZ, Wu HN, Zhang JY, Liu ZH, Li YQ, Luo XL, Lin Y, and Liang R (2017) APE1 overexpression is associated with poor survival in patients with solid tumors: a meta-analysis. Oncotarget 8, 59720–59728 [PubMed: 28938675]
69. Qiushi Wang HX, Qingya Luo, Mengxia Li, Shirong Wei, Xiangfeng Zhu, He Xiao, Lizhao Chen. (2016) Low APE1/Ref-1 expression significantly correlates with MGMT promoter methylation in patients with high-grade gliomas. Int J Clin Exp Pathol 9, 9562–9568
70. Di Maso V, Mediavilla MG, Vascotto C, Lupo F, Baccarani U, Avellini C, Tell G, Tiribelli C, and Croce LS (2015) Transcriptional Up-Regulation of APE1/Ref-1 in Hepatic Tumor: Role in Hepatocytes Resistance to Oxidative Stress and Apoptosis. PLoS One 10, e0143289
71. Kaur S, Ramdzan ZM, Guiot MC, Li L, Leduy L, Ramotar D, Sabri S, Abdulkarim B, and Nepveu A (2018) CUX1 stimulates APE1 enzymatic activity and increases the resistance of glioblastoma cells to the mono-alkylating agent temozolomide. Neuro Oncol 20, 484–493 [PubMed: 29036362]
72. Shkreta L, and Chabot B (2015) The RNA Splicing Response to DNA Damage. Biomolecules 5, 2935–2977 [PubMed: 26529031]
73. Grey M, Dusterhoft A, Henriques JA, and Brendel M (1996) Allelism of PSO4 and PRP19 links pre-mRNA processing with recombination and error-prone DNA repair in Saccharomyces cerevisiae. Nucleic Acids Res 24, 4009–4014 [PubMed: 8918805]

74. Beck BD, Lee SS, Hromas R, and Lee SH (2010) Regulation of Metnase's TIR binding activity by its binding partner, Pso4. Arch Biochem Biophys 498, 89–94 [PubMed: 20416268]

75. Mahajan KN, and Mitchell BS (2003) Role of human Pso4 in mammalian DNA repair and association with terminal deoxynucleotidyl transferase. Proc Natl Acad Sci U S A 100, 10746–10751 [PubMed: 12960389]

76. Onyango DO, Howard SM, Neherin K, Yanez DA, and Stark JM (2016) Tetratricopeptide repeat factor XAB2 mediates the end resection step of homologous recombination. Nucleic Acids Res 44, 5702–5716 [PubMed: 27084940]

77. Marechal A, Li JM, Ji XY, Wu CS, Yazinski SA, Nguyen HD, Liu S, Jimenez AE, Jin J, and Zou L (2014) PRP19 transforms into a sensor of RPA-ssDNA after DNA damage and drives ATR activation via a ubiquitin-mediated circuitry. Mol Cell 53, 235–246 [PubMed: 24332808]

78. Malanga M, Czubaty A, Girstun A, Staron K, and Althaus FR (2008) poly(ADP-ribose) binds to the splicing factor ASF/SF2 and regulates its phosphorylation by DNA topoisomerase I. J Biol Chem 283, 19991–19998 [PubMed: 18495665]

79. Mundle ST, Delaney JC, Essigmann JM, and Strauss PR (2009) Enzymatic mechanism of human apurinic/apyrimidinic endonuclease against a THF AP site model substrate. Biochemistry 48, 19–26 [PubMed: 19123919]

80. Dianova II, Bohr VA, and Dianov GL (2001) Interaction of human AP endonuclease 1 with flap endonuclease 1 and proliferating cell nuclear antigen involved in long-patch base excision repair. Biochemistry 40, 12639–12644 [PubMed: 11601988]

Highlights:

- The mRNA splicing component ISY expression is increased by DNA damage
- ISY1 constitutively interacts with APE1
- This interaction enhances both APE1 binding to abasic sites in DNA and APE1 endonuclease activity
- ISY1 can promote the completion of base excision repair when sub-functional levels of APE1 are present

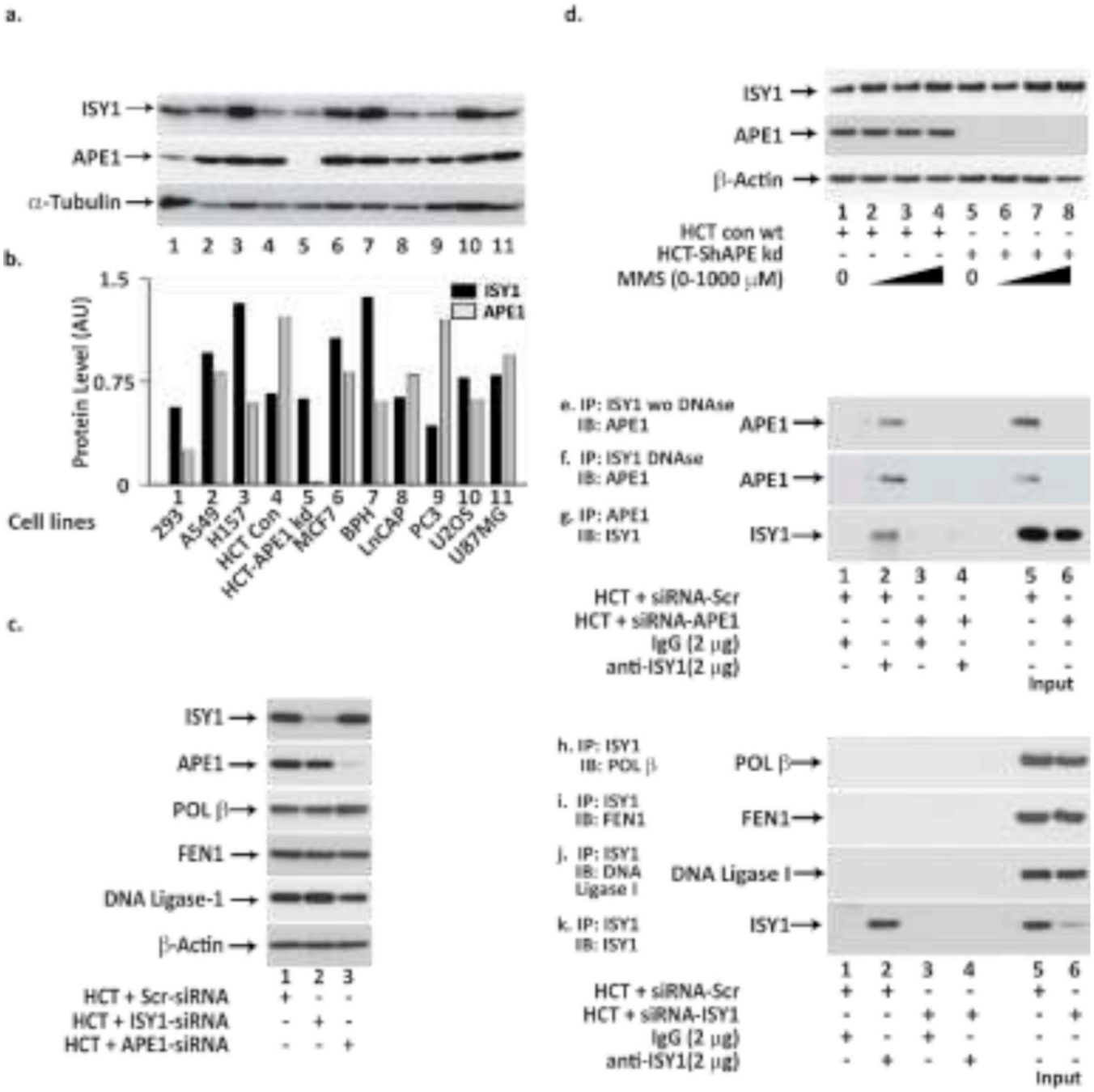

Figure 1. ISY1 levels in various cell lines and its interaction with APE1.

ISY1 protein levels in different cell lines were assessed by western blot analysis. ***Panel a*** shows ISY1 and APE1 protein levels in HEK293, A549, H157, HCT, HCT-APE knock-down, MCF7, BPH, LnCap, PC3, U2OS, and U87MG cells. ***Panel b*** shows quantitation of ISY1 and APE1 after normalization with α-tubulin levels in HEK293, A549, H157, HCT116, HCT-APE1 knock-down, MCF7, BPH, LnCap, PC3, U2OS, and U87MG cells. ***Panel c*** shows the effect of ISY1 and APE1 depletion in HCT116 cells on the level of other

BER proteins. ***Panel d*** shows the effect of varying concentration of MMS (0–1000 μM) treatment on the expression level of ISY1 and

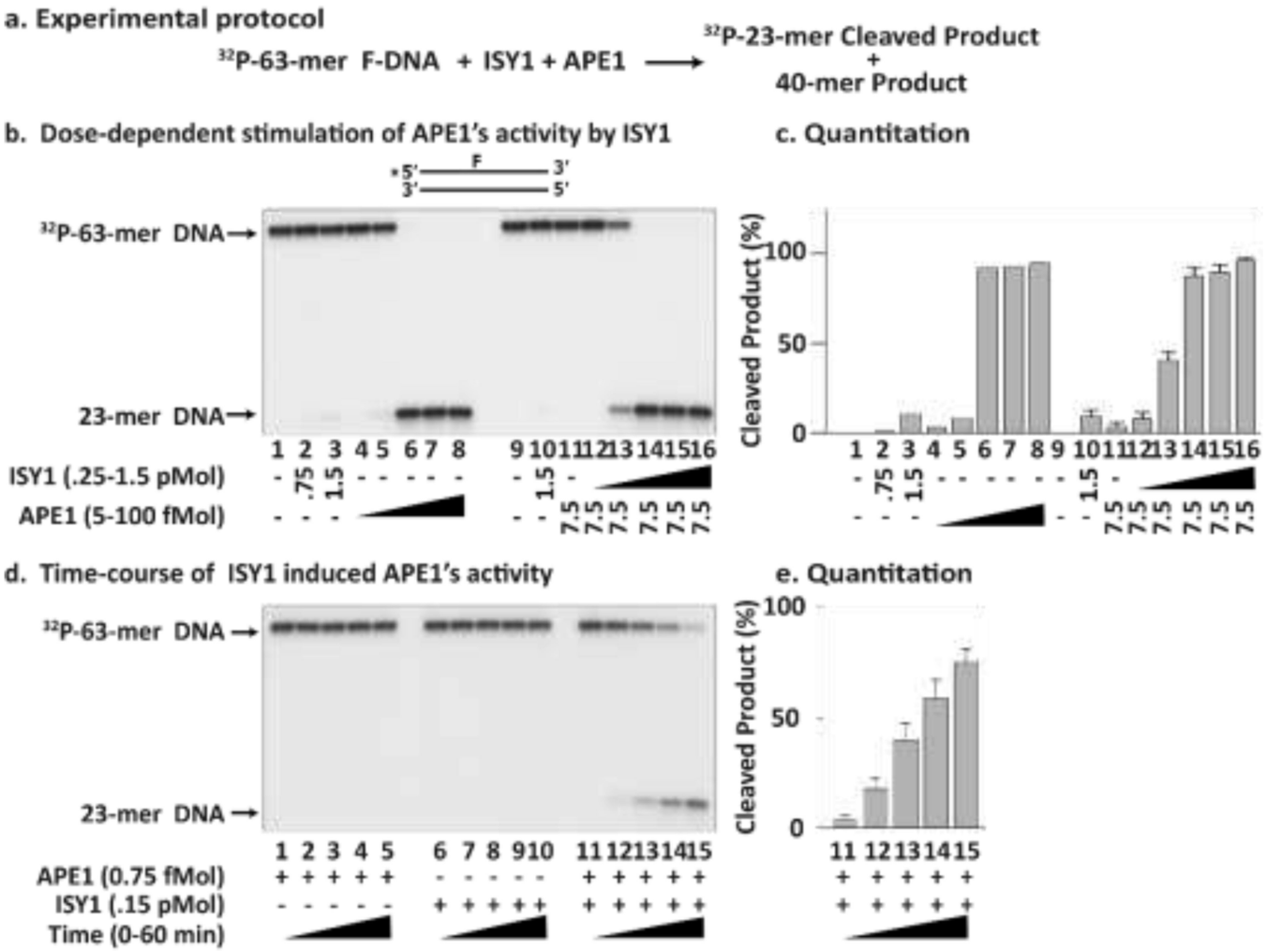

Figure 2. Promotion of the 5' AP endonuclease activity of APE1 by ISY1.

Panel a show the experimental protocol. ***Panel b*** shows the effect of varying concentrations of ISY1 protein on APE1's 5'−3' endonuclease activity on AP-containing double stranded DNA. The top ^{32}P-labeled strand harbors a 3-hydroxy-2-hydroxymethyltetrahydrofuran moiety (F). The incubation time was 45 min. ***Panel c*** shows the effect of time of incubation with limiting amounts of ISY1 and APE1 on the cleavage of 63-mer ^{32}P-labeled F-DNA substrate. The time points were 15, 30, 45 and 60 min. Data are the mean ± SD of three independent experiments.

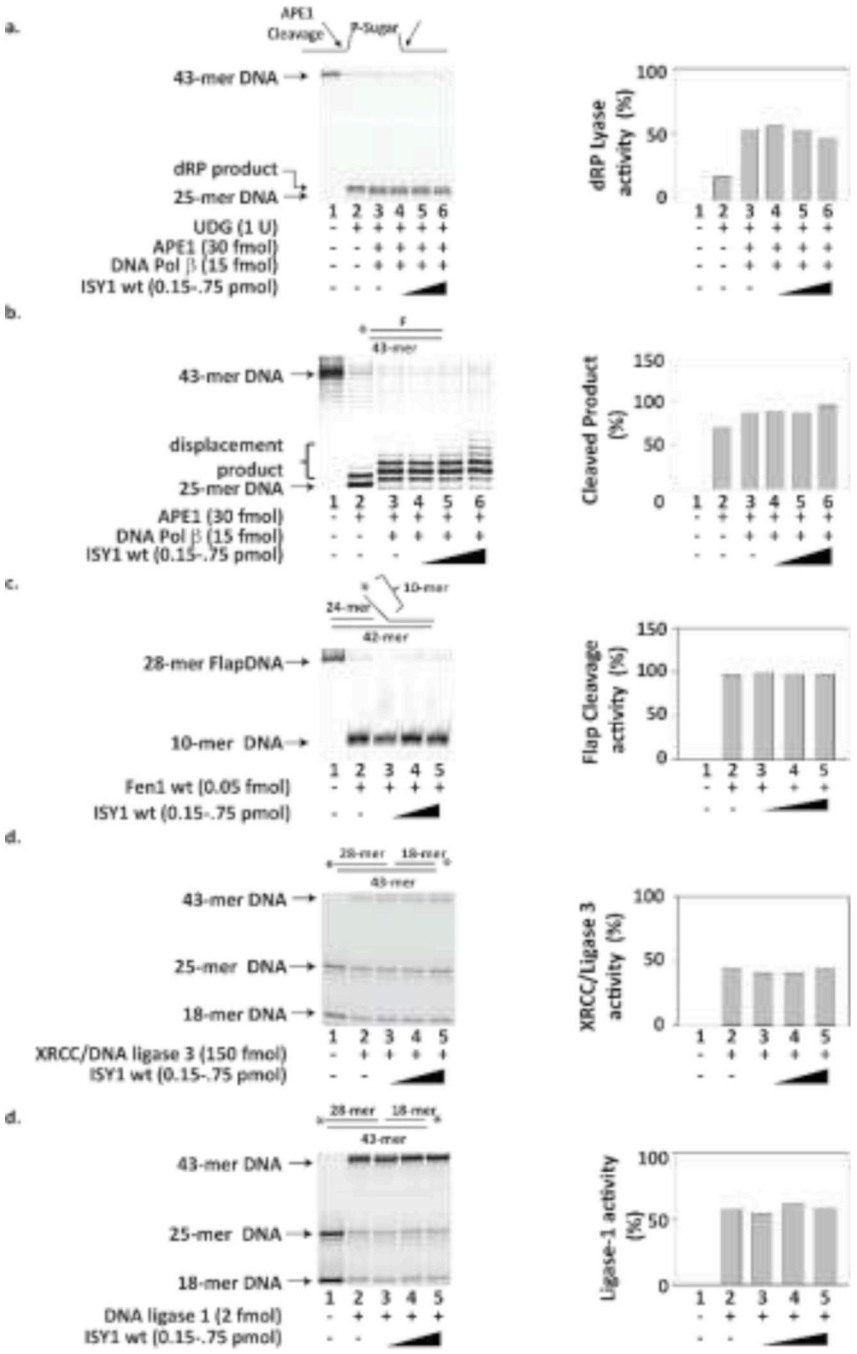

Figure 3. Effect of ISY1 on the dRP lyase activity, Pol β activity, flap endonuclease activity and DNA ligase activity.

Panel a shows effect of varying concentrations of ISY1 on the dRP lyase activity of POL β using U-DNA substrate. The incubation time was 30 min. ***Panel b*** shows effect of varying concentrations of ISY1 on the displacement activity of POL β using abasic-DNA substrate. The incubation time was 45 min. ***Panel c*** shows the effect of varying concentrations of ISY1 protein on flap endonuclease activity of FEN1 using flap DNA substrate. The incubation time was 45 min. ***Panel d*** and ***Panel e*** shows the effect of varying concentrations of ISY1

protein on XRCC/DNA ligase 3 and DNA ligase I activity. Panel on the right side shows quantitation of dRP lyase, POL β, Fen1, XRCC1.Ligase3 and Ligase 1 activity in presence of ISY1. Incubation time for each of the reaction was 60 min and described in materials and method section. Data in the figure is representative of two or more independent experiments.

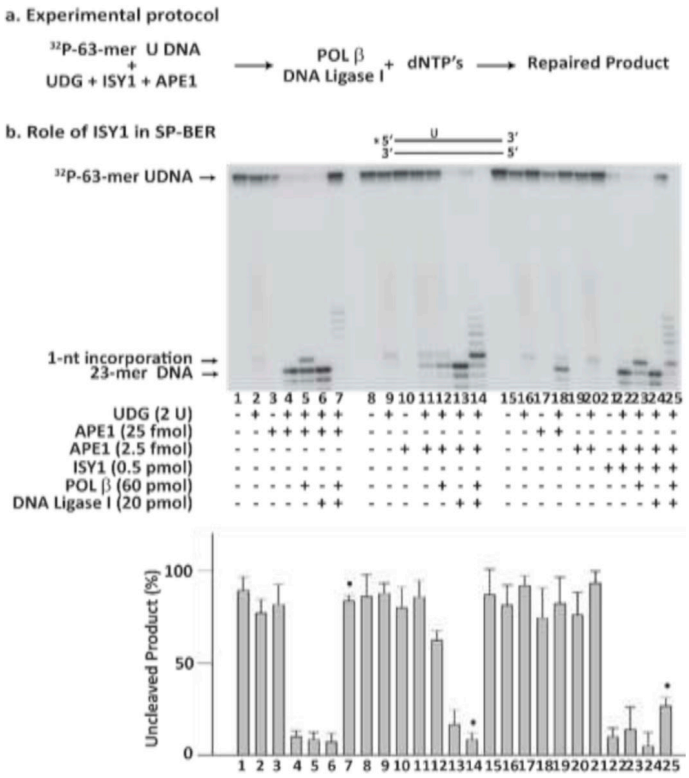

Figure 4. Role of ISY1 in the removal of an uracil residue by SP-BER.

Panel a is the schematic for assembly of the SP-BER reaction system. ***Panel b*** shows the efficiency of ISY1 induced APE1's activity on uracil containing (U) DNA and its processing by the down-stream BER enzymes. The incubation time for reaction was 60 min. Lower panel shows quantitation of uncleaved product representing unrepaired product in absence of DNA ligase 1 and repaired product in presence of DNA ligase 1. * lanes indicate reaction in presence of DNA ligase 1. Data are the mean ± SD of three independent experiments.

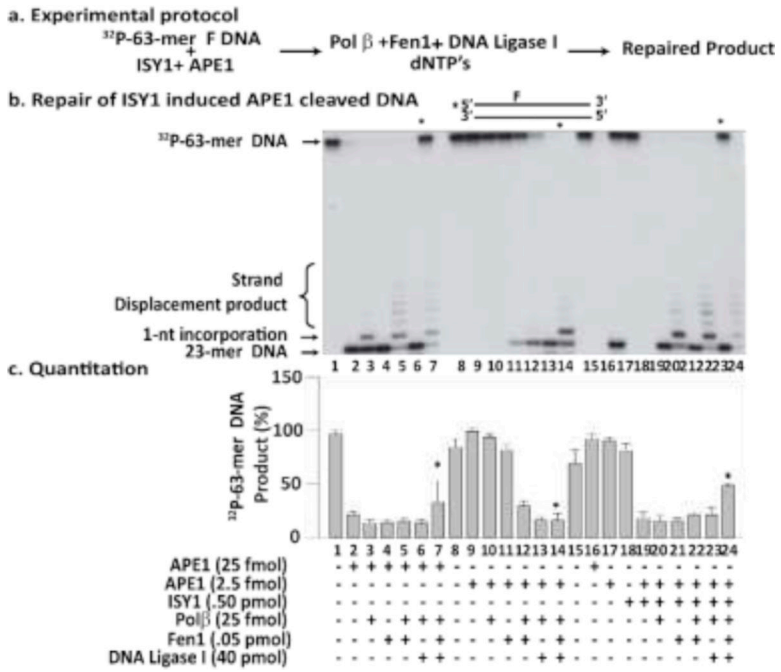

Figure 5. Role of ISY1 in APE1-dependent LP-BER.

Panel a is the schematic representation for assembly of the LP-BER system. ***Panel b*** shows the efficiency of ISY1/APE1 incision at an AP site and processing by down-stream BER enzymes. The incubation time was 60 min. Lane 1 represents ^{32}P-63-mer F-DNA, lane 2 shows 23-mer incised product after excessive APE1 activity, and lane 3 shows displacement activity in the presence of POL β. Lane 5 shows Fen1 stimulated POL β activity, and lane 7 shows the repair of the 63-mer AP site DNA. Lanes 8–14 show a LP-BER reaction in the presence of limiting concentrations of APE1. Lanes 15–24 show the LP-BER reaction reconstituted in the presence of ISY1. Lower panel shows quantitation of uncleaved product representing unrepaired product in absence of DNA ligase 1 and repaired product in presence of DNA ligase 1. * lanes indicate reaction in presence of DNA ligase 1. Incubation time for the reaction was 60 min. Data are the mean ± SD of three independent experiments.

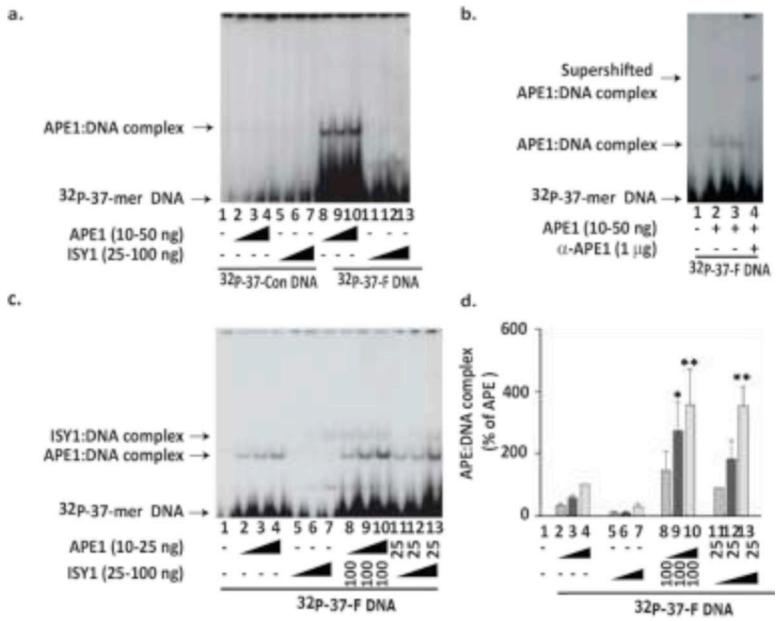

Figure 6. Binding of AP site DNA by ISY1 and APE1.

Binding affinities of ISY1 and APE1 were measured by incubating with ^{32}P-F-DNA. The reaction was assembled on ice and nucleoprotein complexes were resolved on a 5.5% non-denaturing polyacrylamide gel. ***Panel a,*** **APE1** (10–50 ng) **and ISY1** (25–100 ng) were tested for binding either the control or F-DNA. Lane 1, no protein; lanes 2–4, APE1 (10–25 ng); lanes 5–7, ISY1 (10–50 ng) were incubated with ^{32}P-control or ^{32}P-F DNA; lanes 8–10, APE1 (10–25 ng); lanes 11–13 ISY1 (25–100 ng). ***Panel 6b,*** supershifting of the APE1-F-DNA complex by anti-APE1 antibody (2 μg). ***Panel 6c,*** **ISY1 enhances APE1 binding to AP-DNA.** APE1 binding to AP site DNA was assembled on ice. Following the incubation of ^{32}P-F-DNA with APE1 (10–50 ng) and ISY1 (25–100 ng) for 10 min, DNA:Protein complexes were resolved on a 5.5% non-denaturing polyacrylamide gel. The results in ***Panel 6c*** were quantified and plotted. Lane 1, no protein; lanes 2–4, APE1 (25–100 ng); lanes 5–7, ISY1 (25–100 ng) were incubated with ^{32}P-labeled AP site DNA; lanes 8–10, 100 ng ISY1 and varying amount of APE1 (10–25 ng); lanes 11–13, APE1 (25 ng) and varying amount of ISY1 (25–100 ng) were incubated with ^{32}P-labeled AP-DNA. ***Panel 6d*** shows quantitation of the binding of ISY1 and APE1 proteins to AP site DNA. Data are representative of three independent experiments. The arrows indicate the position of free and shifted bands. Data are the mean ± SD of three independent experiments. * $P < 0.05$ and ** $P<0.005$, significantly different than control.

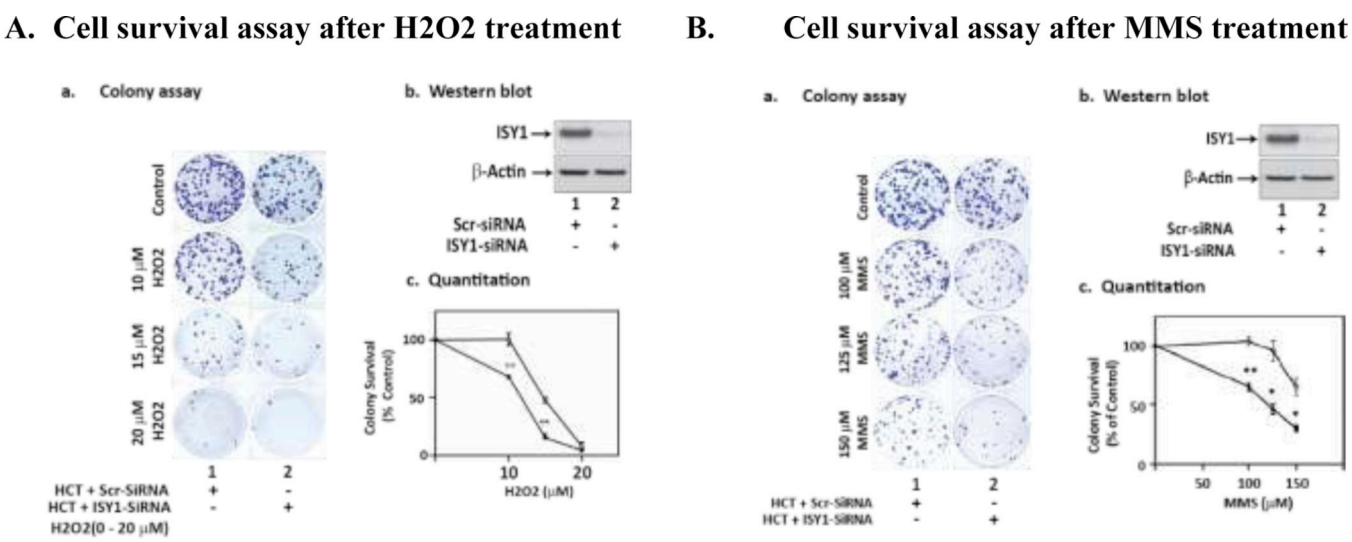

Figure 7. Effect of ISY1 deficiency on survival of HCT116 cells after DNA damage.

Panels A and ***B,*** HCT116 cells were transfected with Scr-siRNA and ISY1-siRNA for 48 h, and then plated for clonal survival assay. After 24 h of plating, cells were exposed to varying concentrations of MMS (panels a-c in A) or H_2O_2 (panels a-c in B), respectively. ***Panels A-a*** and ***B-a*** show representative images of colony survival assay for HCT-116 cells after ISY1-knockdown and then treated with MMS or H_2O_2. ***Panels A-b*** and ***B-b*** show the level of ISY1 in wild-type and ISY1-depleted cells. ***Panels A-c*** and ***B-c*** show quantitative analysis of colony formation after DNA damage. Survival was normalized to cloning efficiency of either ISY1-depleted or scrambled siRNA control cells. Data are the mean ± SD of three independent experiments. * $P < 0.05$, ** $P<0.005$ and *** $P<0.001$, significantly different than control.

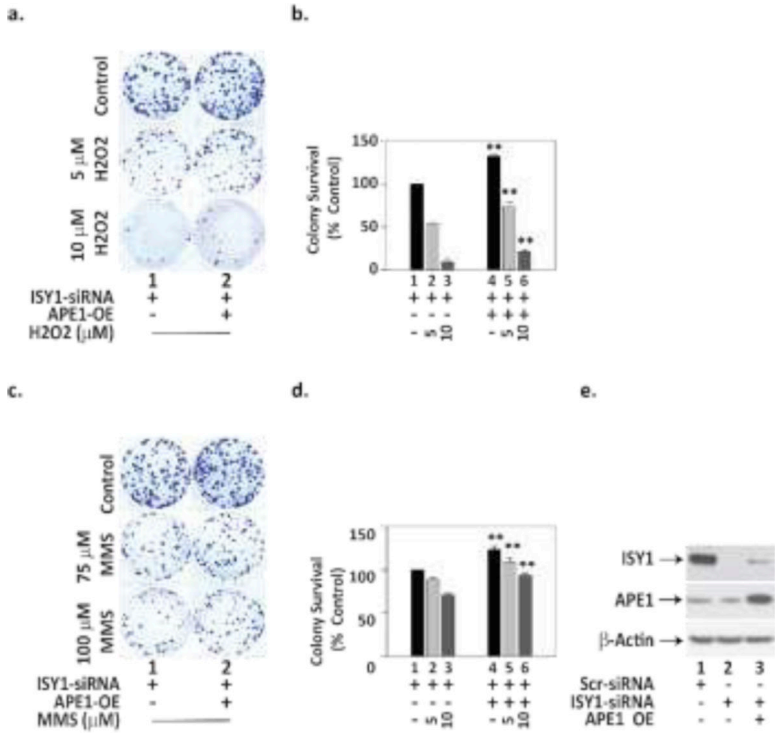

Figure 8. HCT-116 cells depleted of ISY1 are more sensitive to MMS or H_2O_2-induced cytotoxicity as compared to APE1 overexpressed cells.

ISY1 knock-down cells were transfected with Flag-APE1 wt plasmid. Cells were treated with the concentration of 75 and 100 μM of MMS and 5 &10 μM H2O2 for 24 h. After treatment, the medium was replaced with a fresh medium containing 10% (v/v) fetal bovine serum. Cells were allowed to grow till visible colonies are formed. Colonies were stained, counted and analyzed. ***panel a***, colony assay after MMS treatment (representative picture); ***panel b and d***, quantitation of colony assay; ***panel c***, colony assay after H_2O_2 treatment (representative picture). ***Panel e,*** western analysis of ISY1 and APE proteins. β-Actin served as a loading control. Data are the mean ± SD. * $P < 0.05$, ** $P<0.005$ and *** $P<0.001$, significantly different than control.

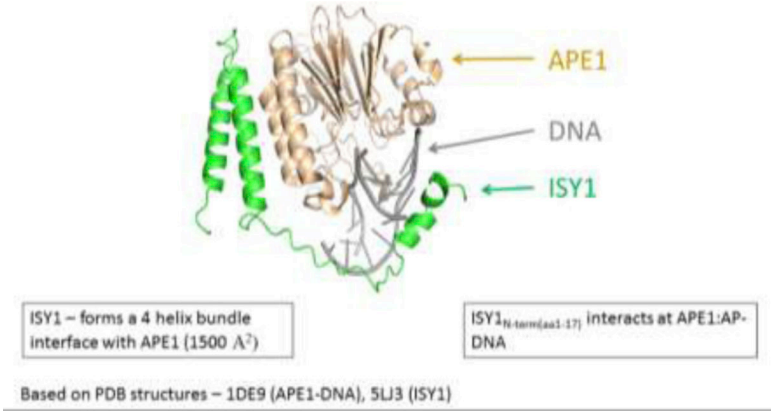

Figure 9. Model of the APE1-DNA-ISY1 complex.

APE1 (wheat), DNA (gray), and ISY1 (green) are shown. The N-terminus of ISY1 wraps around the AP-DNA within the active site of APE1 in a 4-helix bundle, creating a lower energy conformation and stabilizing this complex. The immediate N-terminal aa 1-17 forms two small helices and the two larger helices are formed by aa 40-92.